

UNCLASSIFIED

AD 4 2 5 9 9 0

DEFENSE DOCUMENTATION CENTER

FOR

SCIENTIFIC AND TECHNICAL INFORMATION

CAMERON STATION, ALEXANDRIA, VIRGINIA



UNCLASSIFIED

NOTICE: When government or other drawings, specifications or other data are used for any purpose other than in connection with a definitely related government procurement operation, the U. S. Government thereby incurs no responsibility, nor any obligation whatsoever; and the fact that the Government may have formulated, furnished, or in any way supplied the said drawings, specifications, or other data is not to be regarded by implication or otherwise as in any manner licensing the holder or any other person or corporation, or conveying any rights or permission to manufacture, use or sell any patented invention that may in any way be related thereto.

RTD-TDR-63-3073

RTD
TDR
63-3073

425990

UNCLASSIFIED
AS AD NO. _____

THE CALIBRATION AND INTERPRETATION
OF RECORDED SHOCK-TUBE PRESSURE
DATA USING PIEZOELECTRIC SENSORS

November 1963

TECHNICAL DOCUMENTARY REPORT NO. RTD-TDR-63-3073

Research and Technology Division
Air Force Systems Command
AIR FORCE WEAPONS LABORATORY
Kirtland Air Force Base
New Mexico

Project No. 1080, Task No. 108005

DEC 24 1963

UNCLASSIFIED
TICIA A

(Prepared under Contract AF29(601)-6002 by F. J. Janza,
Research Engineer, and C. W. Hicks, Research Associate
Engineer, of the University of New Mexico at the Air Force
Shock Tube Facility, Alluquerque, New Mexico)

**Research and Technology Division
Air Force Systems Command
AIR FORCE WEAPONS LABORATORY
Kirtland Air Force Base
New Mexico**

When Government drawings, specifications, or other data are used for any purpose other than in connection with a definitely related Government procurement operation, the United States Government thereby incurs no responsibility nor any obligation whatsoever; and the fact that the Government may have formulated, furnished, or in any way supplied the said drawings, specifications, or other data, is not to be regarded by implication or otherwise as in any manner licensing the holder or any other person or corporation, or conveying any rights or permission to manufacture, use, or sell any patented invention that may in any way be related thereto.

This report is made available for study upon the understanding that the Government's proprietary interests in and relating thereto shall not be impaired. In case of apparent conflict between the Government's proprietary interests and those of others, notify the Staff Judge Advocate, Air Force Systems Command, Andrews AF Base, Washington 25, DC.

This report is published for the exchange and stimulation of ideas; it does not necessarily express the intent or policy of any higher headquarters.

Qualified requesters may obtain copies of this report from DDC. Orders will be expedited if placed through the librarian or other staff member designated to request and receive documents from DDC.

FOREWORD

The University of New Mexico greatly appreciates the advice and assistance of Colonel T. J. Lowry, Jr., Captain Thomas F. Dean, and Captain Jack T. Pantall of the Air Force Weapons Laboratory in executing the work performed under Air Force Contracts AF29(601)-4520 and AF29(601)-6002.

Special thanks are due to the following University of New Mexico personnel: Dr. E. M. Zwoyer, Director of the Air Force Shock Tube Facility, for his continuous encouragement and patient consultations; and D. W. Brewer, Research Associate Engineer, for his cooperation in furnishing part of the instrumentation.

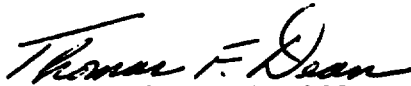
A final word of acknowledgment is given to Mr. Ben Granath of Susquehanna Instruments Company for his contributions in the field of high-performance piezoelectric transducers.


ABSTRACT

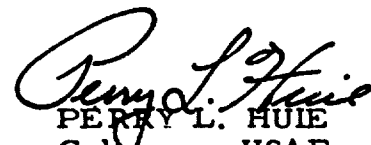
This report is intended to serve as a guide, or basis, for the calibration and analysis of recorded pressure data. Many of the techniques and areas covered are also applicable to other types of gages; i. e., strain, velocity, acceleration, etc. Photographs of typical shock-tube data are generously used to familiarize the reader with the actual appearance of the true pressure pulse which has been modulated by the effects of resonance, overshoot, groundloops, inadequate bandwidth, and poor gage isolation.

PUBLICATION REVIEW

This report has been reviewed and is approved.


THOMAS F. DEAN
Capt USAF
Project Officer


THOMAS J. LOWRY, JR.
Col USAF
Chief, Structures Branch


PERRY L. HUIE
Col USAF
Chief, Research Division

CONTENTS

| | Page |
|---|------|
| Introduction..... | 1 |
| Analysis of pressure sensors for shock tubes and soils... | 6 |
| Analysis of electrically transduced pressure wave... | 6 |
| Calibration of piezoelectric gages..... | 22 |
| Velocity method..... | 22 |
| Reflection check method..... | 27 |
| Pressure-tank method..... | 31 |
| Short-time calibration technique..... | 33 |
| Source and cause of errors..... | 38 |
| Pressure measurements in air and soils..... | 38 |
| Errors introduced by the equipment..... | 39 |
| Fast-rise aspects of pressure pulses..... | 41 |
| Errors introduced by noise sources..... | 44 |
| Noise sources..... | 45 |
| Natural and resonant frequencies..... | 45 |
| Cross sensitivity..... | 51 |
| Mountings..... | 56 |
| Acceleration..... | 58 |
| Groundloops..... | 59 |
| Circuit noise power..... | 62 |
| Temperature variations..... | 65 |
| Cabling..... | 66 |
| Electrostatic effect..... | 68 |
| Appendix A..... | 71 |
| B..... | 72 |
| References..... | 73 |
| Distribution..... | 75 |

ILLUSTRATIONS

| Figure | | Page |
|--------|---|------|
| 1 | Photographs of pressure pulses of three different-size shock tubes..... | 8 |
| 2 | Degradation of shock-wave pressure recording due to improper gage and system characteristics..... | 9 |
| 3 | Pressure-pulse photograph taken in 4-inch shock tube showing resonance and noise effects..... | 10 |
| 4 | Photographs of 4-inch-shock-tube pressure pulse, $\Delta P \approx 12.5$ psi..... | 11 |
| 5 | Charge amplifier (cathode follower) to provide impedance transformation for piezoelectric units and recording system..... | 12 |
| 6 | Diagram of cascade of pressure gage, amplifiers, and recorder..... | 16 |
| 7 | Diagram of square wave generator used to analyze frequency-response characteristics of system..... | 19 |
| 8 | Diagram of a sweep-frequency sine wave generator used to analyze frequency response of system..... | 21 |
| 9 | Calibration of pressure gage by velocity measurement..... | 23 |
| 10 | Short-time calibration method using pressure-tank calibrator..... | 24 |
| 11 | Photographs of 4-inch-shock-tube reflected-pressure pulses for an ST-4 tourmaline gage (traveling-wave principle) which is threaded directly into the steel wall of the shock tube..... | 29 |
| 12 | Photographs of reflected and side-on pressures of gages in, and near, closed end of 4-inch shock tube..... | 30 |
| 13 | Diagram showing details of portable, pressure-tank calibrator..... | 32 |

ILLUSTRATIONS (cont'd)

| Figure | | Page |
|--------|---|------|
| 14 | Photograph of family of pressure curves vs. displacement curves obtained with pressure-tank calibrator, 0 to 70 psi, in 10-psi steps..... | 32 |
| | Graph showing piezoelectric gage output vs. temperature (ST-2)..... | 34 |
| 16 | Diagram of tape recording of calibration pulses applied to the piezoelectric-type gages at gaging stations by short-time calibration method..... | 36 |
| 17 | Diagram showing calibration voltages applied to tape recorder, and photograph of single calibration pulse | 37 |
| 18 | Photographs of pressure pulse in closed-end, 4-inch shock tube, with gages placed in side-on position (b) ahead of and (c) within sand-filled end of shock tube, and sketch of pressure pulses..... | 40 |
| 19 | Diagram of pressure-pulse distortion due to gage and recording system in 2-foot vertical shock tube..... | 43 |
| 20 | Diagram of pressure-pulse change due to response function of gage and recording system (2-foot vertical shock tube)..... | 43 |
| 21 | Errors encountered in calibrating fast-decaying pressure pulses when using pressure-tank method of calibration..... | 44 |
| 22 | Photographs of resonance tests of piezoelectric pressure gages by impulse method..... | 48 |
| 23 | Photographs of resonance tests of piezoelectric pressure gages by impulse method..... | 49 |
| 24 | Four-inch shock tube, transduced pressure pulses at output of low-pass filter..... | 52 |
| 25 | Photographs of shock waves resulting from piezoelectric gages being threaded into and isolated from steel wall of 4-inch shock tube..... | 54 |

ILLUSTRATIONS (cont'd)

| Figure | | Page |
|--------|--|------|
| 26 | Cross-axis sensitivity of piezoelectric gages and decoupling..... | 57 |
| 27 | Distortion encountered by not mounting gage flush with wall of 4-inch shock tube (side-on mounting). | 58 |
| 28 | Photographs of measurement of acceleration noise of a pressure gage..... | 59 |
| 29 | Diagram of typical groundloop found in pressure-measuring system..... | 61 |
| 30 | Removal of periodic noise from tape recording..... | 63 |
| 31 | Temperature variation of the dielectric constant, K , and the piezoelectric strain constants, g_{31} and d_{31} , for PZT-5 ⁴ | 66 |
| 32 | Oscilloscope displacement from pressure gage for constant pressure and different ambient temperatures..... | 67 |
| 33 | Photographs showing (a) pressure pulse from tank calibrator with faulty connector at gage and (b) induced noise voltage from shock wave passing over open connector in gaging station..... | 69 |

1. INTRODUCTION.

The theories underlying the development and application of various gages* used for measuring shock-wave pressures are quite numerous and well documented. However, there is a definite lack of available information which connects the theory with the interpretation of the actual experimental data obtained with these gages. Too often the effects of system noise and distortion are misinterpreted and taken to be the true information presented by the gage; consequently, the purpose of this report is to show the causes which contribute to the recording of false pressure variations which, in turn, introduce errors in the recorded data.

In many cases, the state of the art is not adequately advanced, and distorted pressure data records must be accepted. Here, however, knowledge of the cause of the distortions permits applying justifiable corrections to the data, and some of the data-correction techniques are discussed briefly.

Only a minimum of theoretical information is presented since this aspect of gage development is well covered in the literature; rather, the main effort is concerned with pointing out certain system measurement and calibration methods which give reliable results. The methods of making pressure measurements and attaining accuracy and reliability are covered separately.

The analyses are centered around the application of piezo-electric-type gages for the measurement of shock-wave overpressures

*"Gage" signifies a certain housing using a particular sensing element such as a piezoelectric ceramic, etched foil, etc.
"Transducer" refers, in this report, to a gage, or unit, which changes a pressure/time history to an electrical time history, etc.

generated in different-size shock tubes.* In particular, the piezoelectric sensor and gage assembly are analyzed along with certain pressure-measuring techniques. From actual photographs of shock overpressure, the data are reviewed and compared to indicate the sources of error and the methods available for the reduction of error. It is clearly shown that extraneous information in the recorded pressure/time history can be compensated for or removed by the data-reduction methods. Many of these methods are directly applicable to other gages besides the piezoelectric sensor and gage assembly.

A completely different situation is encountered in making shock-wave (blast) pressure measurements in soils. The measurement of shock pressures in soils (which results from the degradation of a shock wave as it enters the soil and propagates therein) is subject to the very complex phenomena which are involved in the wave propagation from a soil medium to another medium (in particular, the gage mounted in the soil to measure the pressure). In soil studies the presence of a gage may disrupt the free field. One of the effects is a phenomenon known as "arching." This constitutes a redistribution of stress around the gage. Possibly related to this is the imperfect coupling at the boundary between two different media. The electrical analogy is an impedance mismatch. Some of the changes in the electrically transduced signal of the shock wave passing through sand are shown by analysis and experimental data.

The shock waves are generated by three different-size horizontal shock tubes:

(1) A 4-inch-diameter steel tube, 45 feet long, with one end closed: This tube is made of four 10-foot sections and decoupled

* Air Force Shock Tube Facility, Kirtland Air Force Base, Albuquerque, N.M.: Work was done by the University of New Mexico under contracts AF 29(601)-4520 and AF 29(601)-6002.

by rubber O-rings, with one 5-foot section for the compressed air chamber which is used to produce a shock wave of 0- to 20-psi overpressure. (The shock wave is generated by piercing a celluloid diaphragm which releases the compressed air in the 5-foot chamber.)

(2) A 2-foot-diameter steel tube, 200 feet long, with one end closed: This tube is made of ten 20-foot sections, with heavy flanges at each end that permit various sections to be bolted together. (The shock wave is generated by the detonation of primacord to produce an overpressure of 0 to 100 psi.)

(3) A 6-foot-diameter steel tube, 246 feet long, with one end closed: This tube is made of 21 sections, varying from 5 to 20 feet long, with heavy flanges at either end that permit various sections to be bolted together. (The shock wave is generated by the detonation of primacord to produce an overpressure of 0 to 100 psi.)

To obtain the photographed examples of the shock waves shown in this report, the 4-inch tube was used in nearly all cases because it provided a clean, flat-topped shock wave, and because a small tube, easy and inexpensive to operate, is excellent for research.

Two important operations which must be performed to obtain usable stress information for engineering applications are (1) the accurate calibration of the stress gages and their associated recording equipment; and (2) the accurate readout and correct interpretation of the recorded data.

Certain advantages are gained by calibrating the gage in, or by, its "gaging" location (designated as in situ, or in-place, measurements). For this report, a gage calibrated in its actual test environment just prior to and after a shock wave is referred to as an "in-place" calibration. The measurement accuracy made possible by in-place calibration depends largely on the type of

gage being used, the calibration method; the control maintained over such variables as gage placement and the media through which the shock wave propagates; the overall system characteristics (which include amplifier stability and response, cabling effects, groundloops, and signal-to-noise ratios); and the human element. Other pertinent variables are discussed later in relation to a particular gage type.

To verify the calibration of the piezoelectric-type gage and to provide a basis for comparison, three different methods of calibrating a pressure gage are presented: (1) the velocity method, (2) the reflected-pressure method, and (3) the pressure-tank method. It is demonstrated that under controlled conditions of temperature, gage position, etc., the velocity and reflected-pressure calibration methods are accurate within 3 to 5 percent, whereas the pressure-tank method is accurate within 1 to 3 percent.

For analysis of the gage outputs, "noise" is defined to include noise contributions due to (1) mechanical resonance, (2) cross-axis pickup, (3) temperature variations, (4) groundloops in the recording system, (5) improper gage isolation, and (6) the signal amplifying and recording system. Also analyzed is the unwanted modification of the pressure/time history (transformed to a voltage variation) due to these noise-generating sources in the entire pressure-sensing area and in the readout system. Such noise sources modulate the desired information. If the noise components are not identifiable, the data are, unknowingly, in error; if the noise components are identifiable, data-reduction methods can be used to improve the accuracy of the data. Pressure/time histories obscured by noise are generally found to be in the low-level signal range. Methods can be applied to the recorded low-level signal which improve the signal-to-noise ratio.

A limited number of comparisons are made of the piezoelectric gage with other types of gages which use different pressure-sensing elements. Resistive, piezoresistive, piezomagnetic, piezoelectric, electromagnetic, capacitive, and mechanical sensors can be used for stress measurements. (This by no means exhausts the various type sensors which are or can be utilized for measuring stress. See appendix A for some of the pressure gages analyzed in this report. Appendix B is a more complete display of gages which are used for measurement of displacement, pressure, acceleration, and strain. These are some of the gages used for the study of shock wave effects on structures in air and soils.)

This report emphasizes sensors having very wideband, frequency-response characteristics which can closely follow the extremely fast rise time (less than $0.01 \mu\text{sec}$) and the slow decay (10 to 300 msec) of shock-wave pressures in gas media. The low- and high-frequency response features of the entire gaging system (gage plus amplifiers and recorders) are analyzed and compared in photographs of typical shock-wave pressure/time histories of the 4-inch, 2-foot, and 6-foot shock tubes. Some photographs show certain pertinent aspects of a slow-rising pressure wave (0.2 to 10 msec), such as those encountered in the attempted measurement of pressure waves in soils which shows the pulse stretching of the air blast-induced wave by such media. Perhaps mechanical and electrical analogies can be made of soil media.

2. ANALYSIS OF PRESSURE SENSORS FOR SHOCK TUBES AND SOILS.

Shock-wave overpressures in gases have been measured using various types of sensors which utilize mostly the piezoelectric materials (quartz, barium titanate ceramics, tourmaline, etc.) and strain-gage elements (both resistive and piezoresistive). The characteristics of some of these sensors are given in the references.¹⁻⁷ To be able to reproduce closely, and generally electrically, the very fast rise and the following slow pressure drop places stringent design requirements on these sensors. Many gages are excited into resonance by the rapid-rise, pressure-step characteristics (impulse-type excitation) of the shock wave. The need to improve the high-frequency response characteristics of the pressure sensor has forced the gage designer to reduce the size of the sensing element. This serves two important purposes: (1) it reduces the transit time of the pressure pulse across the face of the sensing element when it is placed in a "side-on" position (reads incident pressure, no reflected component); and (2) it raises the natural resonant frequency of the sensor element. (This does not mean that the resonant frequency of the sensor is influenced by the housing.) This adversely lowers the electrical output which usually cannot be tolerated, particularly when the shock-wave pressure levels being measured are low; consequently, for low pressures, fast gage response is not commensurate with large signal outputs. In addition, low signal generation caused by low driving pressures is objectional since the signal is usually modulated by the noise in the system which usually has amplitudes of the same order as the signal.

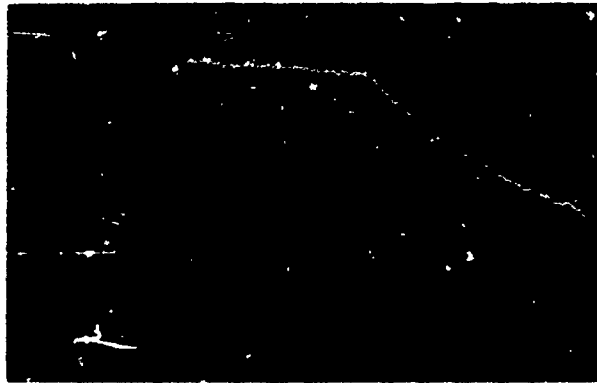
a. Analysis of electrically transduced pressure wave.

The rise time, T_r , for a "cleaned-up" shock wave (plane wave front) is almost instantaneous. There is a fast-rise portion and a sustained constant pressure (flat region) of the shock wave; the latter depends on the size of the shock-wave generating chamber

(particularly the length). The rise, flat-top (not apparent on all photographs because of the short duration, less than 1 msec), and falloff portions of typical shock waves traveling in a shock tube are depicted in the photographs shown in figure 1 for three different-sized shock tubes, as described in a report by Crist and Holt,⁸ where piezoelectric-type gages were used to sense the pressure variations. The pressure-pulse oscilloscope traces shown in figure 1 were obtained with a 4-inch shock tube (shock wave generated by bursting a retaining diaphragm on a compressed air chamber 5 feet long); and a 2-foot and 6-foot shock tube (shock wave in each generated by the detonation of primacord placed on racks of various lengths). The ideal gage, including the associated amplifying and recording system, should follow the pressure profile without overshoot, and not be appreciably modulated by resonance, acceleration, or cross-axis signals. These deleterious effects which distort the pulse-type, pressure/time data are presented in the pressure-pulse drawing, figure 2. For comparative purposes, the resonance and overshoot effects are shown in a photograph (fig. 3) of an actual pressure/time history. Figure 4 is the same pressure/time history but with the time base expanded by a factor of ten; the upper photograph is for the gage in a rubber isolating mount, and the lower photograph for the gage in a nylon isolating mount.

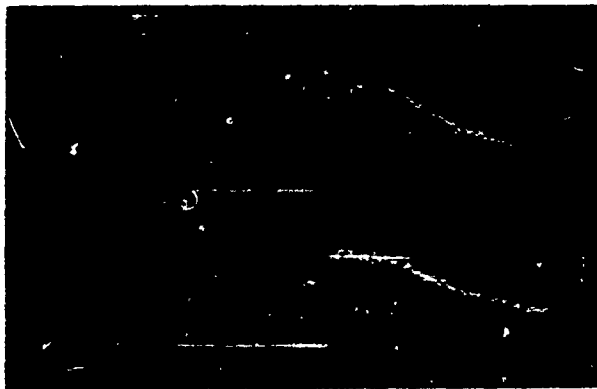
The detection of excessive error in the droop of the flat-top and decay regions is not readily apparent from observation of the photographed pressure data and requires a careful analysis of the overall measuring system. Droop is usually a function of the amplifiers, seldom of the sensors; however, a faulty gage responds the same as one with an output shunted by a low resistance. (Air leaks due to poor sealing or mounting of the gage, or low leakage resistance give such results.)

The error in the droop region of the pressure pulse can be almost completely eliminated by a "charge" amplifier (cathode



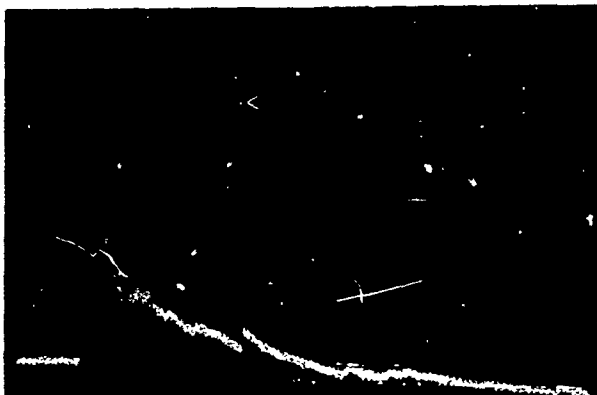
Gage: ST-2, rubber isolator
 Sensor: lead metaniobate
 Sweep: 2 msec/cm
 Displacement: 0.2 v/cm
 Rise time: 5 μ sec (cathode
 follower ac-coupled
 to Tek. 551 scope)
 Flat top: 7 msec
 Decay: 12 msec

a. Four-inch-shock-tube pressure pulse, $\Delta P \approx 12.5$ psi



Gage: ST-2, nylon isolator
 Sensor: lead metaniobate
 Sweep: 5 msec/cm
 Rise time: 5 μ sec (cathode
 follower ac-coupled
 to Tek. 551 scope)
 Flat top: 7 msec
 Decay: 70 msec

b. Two-foot-shock-tube pressure pulse, $\Delta P \approx 50$ psi



Gage: ST-2, nylon isolator
 Sensor: lead metaniobate
 Sweep: 50 msec/cm
 Displacement: 200 mv/cm
 Rise time: 15 μ sec (cathode
 follower dc-coupled
 to tape recorder)
 Flat top: 3 msec
 Decay: 180 msec

c. Six-foot-shock-tube pressure pulse, $\Delta P \approx 60$ psi

Figure 1. Photographs of pressure pulses of three different-size shock tubes

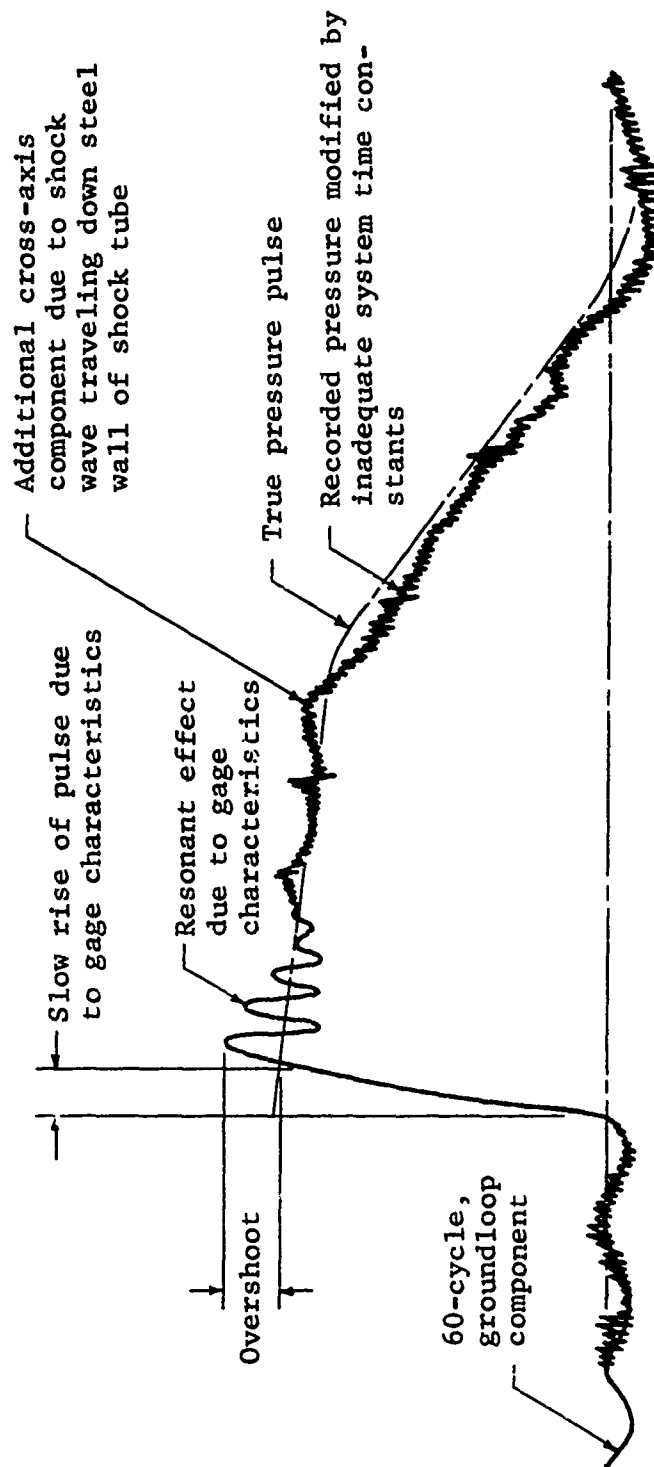
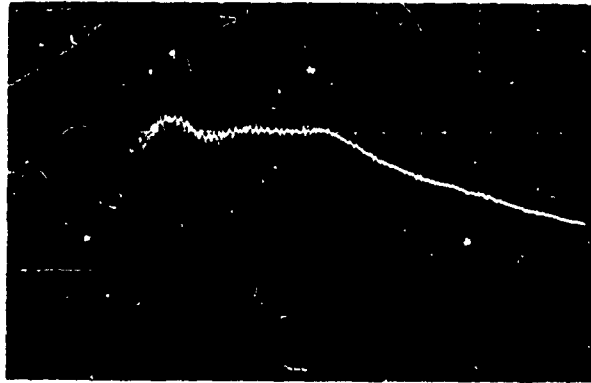


Figure 2. Degradation of shock-wave pressure recording due to improper gage and system characteristics



Sweep: 2 msec/cm
 Displacement: 0.2 v/cm
 Isolator: rubber grommet

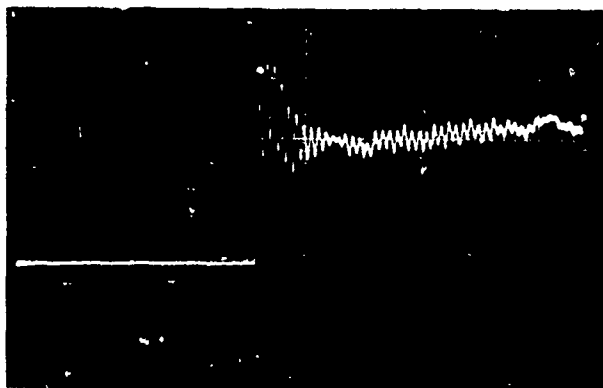
Figure 3. Pressure-pulse photograph taken in 4-inch shock tube showing resonance and noise effects

follower) which has an extremely long time constant in the input stage being fed by the piezoelectric gage. The resistance factor of the time constant which prevents excessive rates of charge leakage is of the order of 10^{11} ohms. Time constants of the order of 10 sec, or more, are readily attained. Direct coupling in the following amplifier stages provides the required low-frequency response:

The first of these requirements is made possible by an electrometer tube in a basic cathode-follower stage as shown in figure 5. The input time constant, τ_{in} , of the cathode follower is given by RC . A typical value for τ_{in} , for the gage and the associated cable* from the gage to the cathode follower, is given by

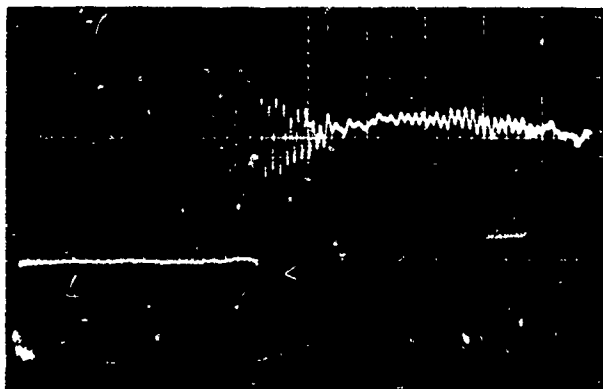
$$\tau_{in} = R_1 \times (C_g + C_c) \quad (1)$$

*Special, low-noise coaxial cable is used, having a graphite layer between the braid and rubber cover to reduce electrostatic pickup (trade names of Microdot and Mininoise).



Gage: stretched diaphragm
 Isolator: rubber grommet
 Sensor: quartz
 Sweep: 0.2 msec/cm
 Rise time: 5 μ sec (calibration amplifier
 dc-coupled to Tek.
 551 scope)
 Flat top: 7 msec
 Decay: 12 msec

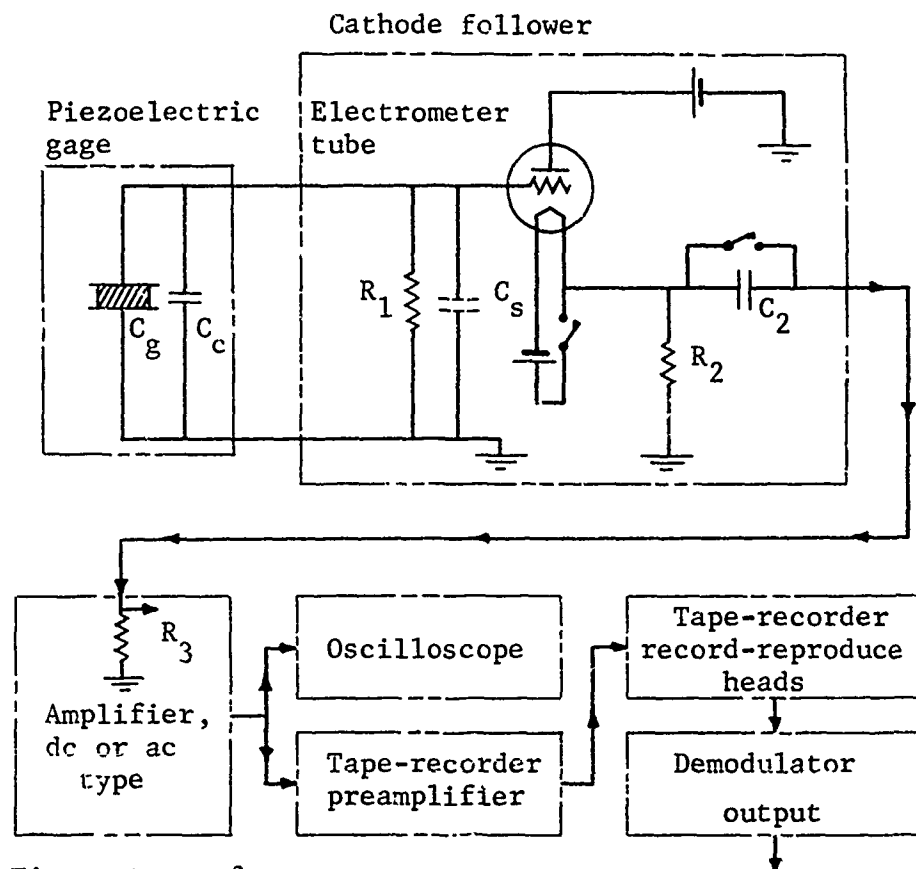
a. Pressure pulse with rubber grommet



Gage: stretched diaphragm
 Isolator: nylon grommet
 Sensor: quartz
 Sweep: 0.2 msec/cm
 Rise time: 5 μ sec (calibration amplifier
 dc-coupled to Tek.
 551 scope)
 Flat top: 7 msec
 Decay: 12 msec

b. Pressure pulse with nylon grommet

Figure 4. Photographs of 4-inch-shock-tube pressure pulse,
 $\Delta P \approx 12.5$ psi



First stage of amplification

$$R_1 \approx 10^{11} \text{ ohms}$$

$$R_2 = 2 \times 10^4 \text{ ohms}$$

$$R_3 = 10^6 \text{ ohms}$$

$$C_c \approx 100 \text{ pf (picofarads)}$$

$$C_g \approx 250 \text{ to } 3,000 \text{ pf}$$

$$C_s = \text{variable, } 10 \text{ to } 5 \times 10^4 \text{ pf}$$

$$C_2 = 5 \text{ } \mu\text{f (microfarads)}$$

$$(C_1 = C_g + C_c + C_s)$$

Figure 5. Charge amplifier (cathode follower) to provide impedance transformation for piezoelectric units and recording system

where $R_1 \approx 10^{11}$ ohms, $C_g = 250$ to $3,000$ pf (picofarads), $C_c = 100$ to $1,000$ pf (20 to 30 pf per foot of cable). (Additional shunt capacitance, C_s , can be added to control the input voltage level to the electrometer tube; thus, the total capacitance would be $C_1 = C_g + C_c + C_s$.) Thus, for a representative value

$$\tau_{in} = 10^{11} \times (3,000 + 1,000) \times 10^{-12}$$

$$\tau_{in} = 400 \text{ sec}$$

From this example, it is apparent that the droop region of a long pressure pulse is not affected by the leakage path provided by the input shunt resistance which is the larger factor in the input time constant, τ_{in} ; consequently, any appreciable distortion which is introduced is mostly the result of inadequate low-frequency characteristics of the cathode follower and the remaining amplifying and recording system. Direct coupling throughout the entire system, from sensor to recorder, provides the ideal arrangement for reducing low-frequency error; however, the drift inherent in dc coupling, particularly on a long time basis, is objectionable when a large number of gages are used in involved tests.

Most of the drift is due to the temperature gradients which shift the dc level of the input to the cathode follower. This can be eliminated by resorting to ac coupling of the cathode follower to the input of the following amplifier. Referring to figure 5, the output time constant, τ_{out} , is given by

$$\tau_{out} = (R_2 + R_3) C_2 \quad (2)$$

where for typical values

$$\tau_{out} = (2 \times 10^4 + 10^6) 5 \times 10^{-6}$$

$$\tau_{out} = 5.1 \text{ sec}$$

For example, with a 200-msec, square pulse input (this would represent a long duration, positive-phase shock wave, such as is encountered in the 6-foot tube), the voltage drop for the time constant in equation 2 is given by

$$E_1 = E_0 e^{-t/\tau_{out}} \quad (3)$$

where, for the values shown for R_2 , R_3 , and C_2 , $E_1 = 0.96 E_0$. This time constant introduces an error of 4 percent at the end of the 200-msec interval. (Leakage resistance must be exceptionally high for capacitor C_2 to prevent developing an excessive dc-offset voltage in the input of the following high-gain dc amplifiers usually encountered in actual operations.)

The piezoelectric ceramics are popular sensing materials for use in gages measuring shock pressures in gases because of high sensitivity (small-sized sensors allow fast rise times with reasonable charge outputs per psi, pQ/psi, where pQ = picocoulombs); ruggedness; stability; good aging properties; adequate temperature range; and the excellent property of linear charge output versus pressure (coulombs [Q] versus psi) over a range of 0 to 1,000 psi. Strain-gage elements in half- and full-bridge arrangements cemented onto a small diaphragm (less than 1/2-inch diameter) and placed into

the gage housing are applicable for impulse (pressure x time) measurements; however, this gage has low resonant-frequency characteristics, under 30 kc, and shock excitation causes ringing. Being delicate, this gage cannot stand much overload. Piezoresistive elements made from P- and N-type, silicon, semiconductor materials are now being more frequently used for such type gages.^{9,10} These elements introduce very low acceleration modulation and extremely low cross-axis pickup because of their small mass and small cross-sectional area. The high-frequency response extends to 35 kc for the piezoresistive gages; whereas, in comparison, frequency response is as high as 300 kc for the ceramic-type piezoelectric gages. Their low-frequency response characteristics are also comparable.

The fast-rising shock front is delayed by the piezoelectric transducer because of its slower response time when it is placed in a side-on position for making a pressure measurement. In the side-on position, the shock wave is integrated as it passes across the sensor face. The response time is largely a mechanical problem since reducing the diameter of the sensing element reduces the transit time of the shock wave across the face of the sensor. Sensing elements, 1/16- to 1/8-inch in diameter, have rise times around 3 to 8 microseconds.

To have distortionless reproduction of the transduced voltage output of the sensor for the fast and slow pressure variations requires an overall, wideband system extending from dc to 50 kc, or more. Such a system is depicted by the block diagram in figure 6. Here, a cascade is shown of a piezoelectric gage, cathode follower, high-gain dc amplifier, and a tape recorder (including its own driving amplifiers) or a galvanometer. Associated with each unit of the cascade is a gain function, $G_i(f)$, and a bandwidth, B_i . The gain and bandwidth of each unit in the cascade

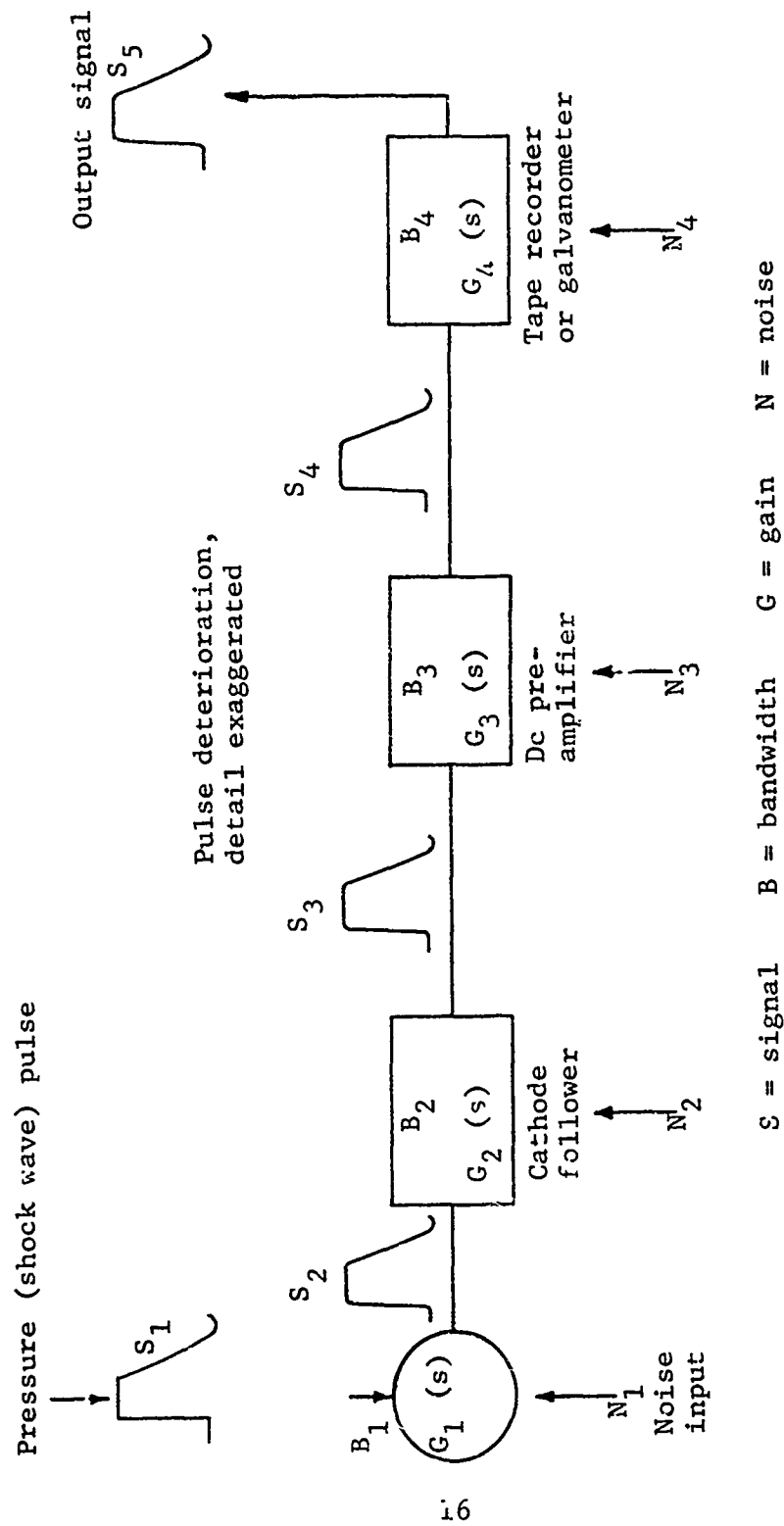


Figure 6. Diagram of cascade of pressure gage, amplifiers, and recorder

enters into the determination of the amount of distortion added to the true shock-wave pressure pulse (the pressure wave is changed by the transducer to an electrical voltage) as it travels in its converted voltage form through the entire system. Figure 6 indicates that the distortion developed by each stage can be treated separately. The distortion can be the result of the narrowing of the overall bandwidth by cascading and by the addition of noise, N_i , by each stage.

It is necessary to know the gain function, $G_i(f)$, for each unit of the cascade. From the gain function of a single stage the bandwidth characteristics can be found. It cannot be assumed from a particular $G_1(f)$ that the bandwidth characteristics of the entire system can be found; nor can it be assumed that $G_1(f)$ is constant over an entire bandwidth. (The bandwidth given is between the low- and high-frequency points which are down 3 db from the mid-band gain.)

First, consider the piezoelectric gage in the cascade. This unit is generally designated as a transducer since it converts pressure, $P(t)$ where t = time, into a charge output, $Q(t)$, where volts, $V(t) = Q(t)/C_T$ (C_T = total shunt capacitance of the input). Experimental data readily verify that for most piezoelectric gages Q is directly proportional to P over a large pressure range, provided the temperature, T , and frequency, f , are held constant.

Actually no value is determined for the gain, $G_1(f)$, for a transducer; it is important to note that, to a small degree, the gage gain is a function of frequency. But it is better to think of this dependence in terms of response time, T_r . For example, the overshooting and ringing of a gage is a function of the high-frequency components in the applied pressure wave. (See fig. 4.) A nonovershooting, nonresonating response of a gage to a pressure wave is a good indication that the gage has a uniform frequency response

throughout an adequate bandwidth.

In contrast, the low-frequency characteristics of a gage can be observed. This is accomplished by a solenoid-operated valve on a pressure tank which is used to apply pressure to the gage. The solenoid has a slow response, thus applying the tank pressure to the gage in about 2 to 10 msec; the pressure in the tank is then maintained on the gage. The frequency components that make up the pressure profile are therefore in the range of approximately 0 to 100 cycles per second.

The indicated pressure level related to the gain function is essentially constant throughout the bandwidth. The application of an impulse by head-on excitation (pressure applied that is normal to sensing element-reflected pressure) sets the gage into resonance from which the upper frequency limit can be derived. These measurements, though not continuous, provide the necessary information on response characteristics.

The gage and bandwidth of the individual units, the cathode follower, the amplifier, and the recorder can be measured by standard laboratory methods, or can be obtained from the manufacturer's specifications; however, the response measurements of the overall system are more informative.

The technique of applying a square wave generator to the input of the cascade and then observing the output which gives more rapidly an indication of the expected pulse deterioration both in the low- and high-frequency regions (fig. 7) is preferred to the involved and laborious process of experimentally plotting the frequency response of the system by a point-by-point method. The low response is maintained by using dc amplifiers throughout the system except, possibly, for the first stage (cathode follower) of the cascade which is ac coupled to avoid the drift problem. So as not to retard excessively the fast rise of the shock wave (appearing

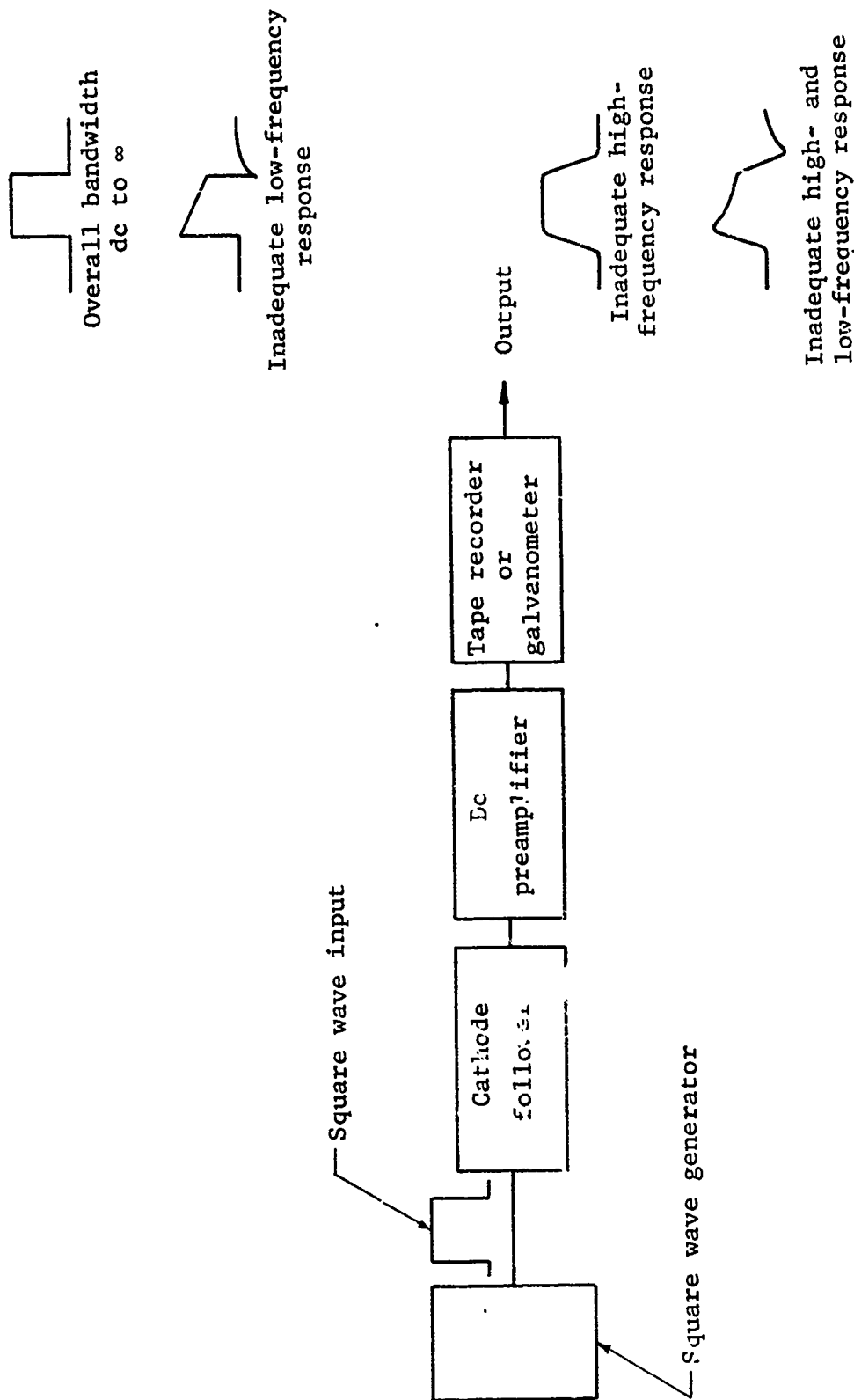


Figure 7. Diagram of square wave generator used to analyze frequency-response characteristics of system

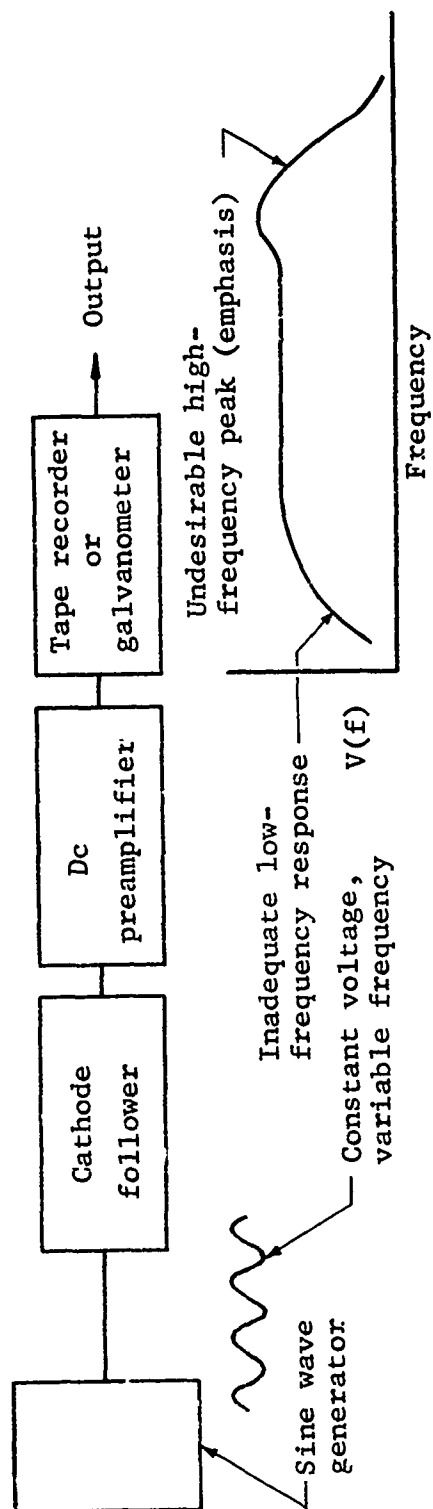


Figure 8. Diagram of a sweep-frequency sine wave generator used to analyze frequency response of system

3. CALIBRATION OF PIEZOELECTRIC GAGES.

Various methods of calibrating piezoelectric gages for pQ versus psi have been used. Under the same test conditions, excellent agreement has been obtained by using three methods of calibration which we will designate as (1) the velocity method, (2) the reflection check method, and (3) the pressure-tank method. Of these three, the pressure-tank method has been the most instrumental in reducing error in the recorded data by making it practical to take calibrations prior to, and directly after, the recording of the shock-wave overpressure.

a. Velocity method.

The velocity method was probably the first and most popular method in the calibration of gages used for shock-tube pressure measurements. Calibration is dependent upon accurate measurements of the shock-front velocities throughout a range of overpressures. These velocities are substituted in the usual expression for overpressure resulting from the application of the Rankine-Hugoniot relations as found in Wright.¹³ The shock wave is usually generated in a small-diameter shock tube (2- to 4-inch-diameter pipe) where the shock wave is formed by piercing the retaining diaphragm of an air chamber at pressures ranging from approximately 10 to 150 psi (fig. 9). This yields overpressures ranging from 4 to 25 psi. Figure 10 shows a schematic of the 6-foot shock tube where gaging stations 2 and 3 can be used to record the velocity of the shock wave. Approximately 6-tube diameters away from the compressed air chamber, the shock front is "cleaned up" and the Rankine-Hugoniot equations for usually encountered or low-strength shock waves apply. Thus, the expression for shock Mach is given by

$$M = \frac{U}{C_0} = \left[\frac{\gamma + \mu}{1 + \mu} \right]^{1/2} \quad (6)$$

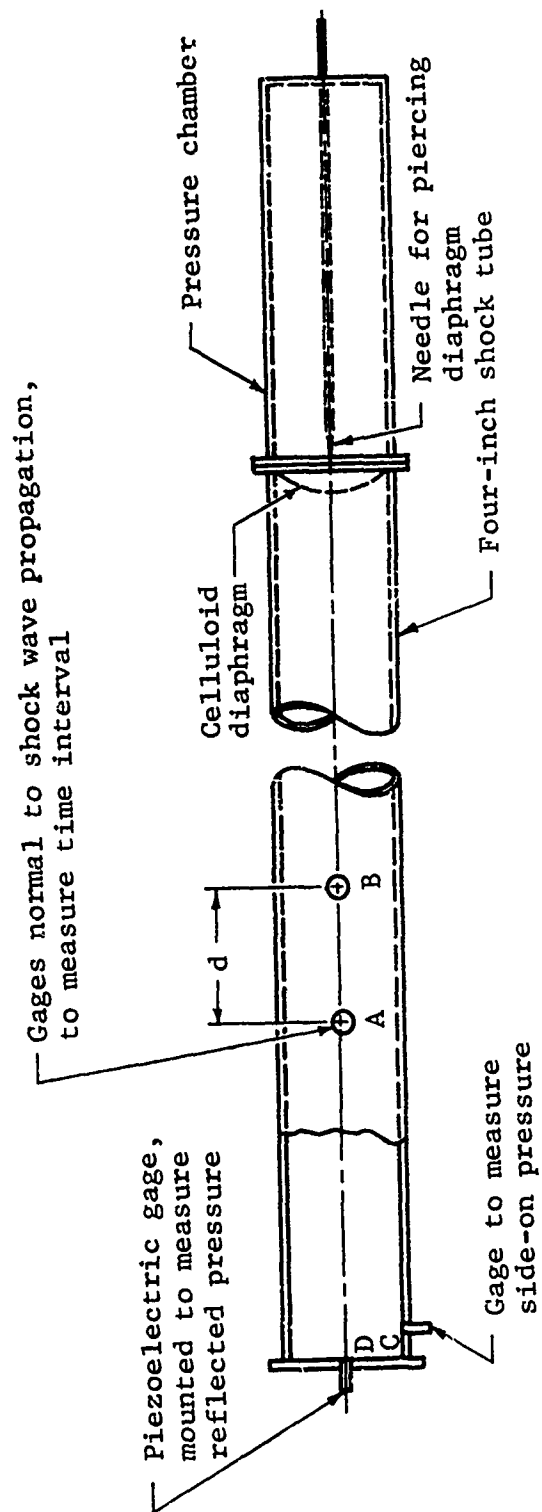


Figure 9. Calibration of pressure gage by velocity measurement

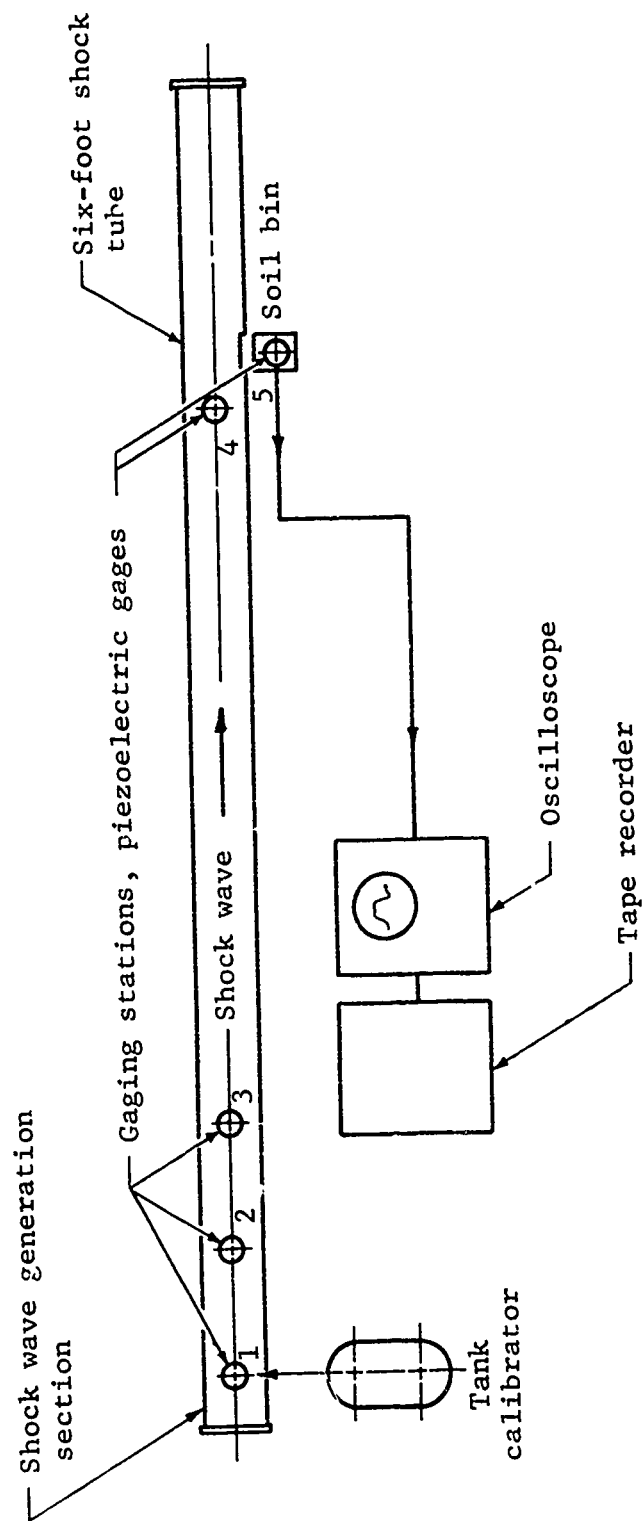


Figure 10. Short-time calibration method using pressure-tank calibrator

where

C_o = sonic velocity in a gas, or gas mixture, at test pressure, temperature, and humidity;

U = shock velocity; and

$y = \frac{P_1}{P_o}$. P_1 is the absolute pressure; and P_o is the pressure ahead of the shock front.

For example,

$$C_o = \left[\frac{\gamma P_o}{\rho_o} \right]^{1/2} \quad (7)$$

where ρ_o is the density ahead of the shock front and

$$\mu = \frac{\gamma - 1}{\gamma + 1}, \quad \gamma = \frac{C_p}{C_v}, \quad \text{or } \gamma = \frac{7/6}{5/6} = 1.4 \text{ for air.}$$

(C_p = specific heat at constant pressure; C_v = specific heat at constant volume.)

The expression for measured overpressure is ΔP , where $\Delta P = P_1 - P_o$, and is given by

$$\frac{\Delta P}{P_o} = \frac{7}{6} (M^2 - 1) \quad (8)$$

To determine ΔP , it is first necessary to measure U , C_o , and P_o . The shock velocity, U , is measured in the 4-inch shock tube over as small a distance interval, d , as possible (usually 1 foot), but a distance which still gives good resolution in the time interval, Δt , when using an electronic time-interval counter, figure 9. The usual time resolution with a counter is one μsec , or better. The time interval is measured by using piezoelectric gages

which, when placed in a side-on position in the shock tube, sense the incident pressure, at points A and B shown in figure 9.

The sonic velocity, C_o , for air can be obtained from charts which include effects of temperature and humidity to an accuracy of about 1 percent. A more accurate, but possibly more involved, method of obtaining C_o is to measure the travel time of a short sound pulse in the shock tube. This can be done with a sound source at one end of the tube and a pickup at the other end. Variations in effects of air density and humidity are included in this type of velocity measurement.

The static pressure, P_o , is determined directly from a barometer reading.

Substitution of U , C_o , and P_o in equation 8 yields ΔP .

The disadvantages of this method are as follows:

- (1) measurements of U require the critical adjustment of the voltage levels to actuate the counter throughout the measured overpressure range, ΔP , particularly for sensor installations which are subject to high cross-axis excitations;
- (2) for each overpressure evaluation, readings of U , C_o (function of temperature and humidity), and P_o are required;
- (3) a plot of ΔP versus picocoulombs, pQ , is required for about seven points to prove the linearity of the gage and to check the scatter in the data;
- (4) the range of overpressures is severely limited by the pressure attainable in the compressed air chamber; and

- (5) the method is time consuming, even with the aid of a special calibration facility.

b. Reflection check method.

Another method of pressure calibration which provides a valuable check on other calibration methods is the measurement of reflected pressure. The equation applicable to reflected pressures is found in Wright¹³ and is given by

$$\frac{\text{Reflected overpressure}}{\text{Incident overpressure}} = \frac{P_2 - P_o}{P_1 - P_o} = \frac{(2\mu + 1)y + 1}{\mu y + 1} \quad (9)$$

where

$$\mu = \frac{\gamma - 1}{\gamma + 1}, \quad \gamma = \frac{C_p}{C_v}$$

($\gamma = 1.4$ for air, thus $\mu = \frac{1}{6}$), and

$$y = P_1/P_o \text{ (shock strength)}$$

This method requires a control gage which has a high-frequency response and does not ring when excited by a step function such as that presented by the shock wave normally incident on the gage (head-on). (If the high response is inadequate, a low-pass filter can be used to eliminate the ringing component.) Gages*

*"Susquehanna Instruments, Bel Air, Md. ST-4 Specs: See Appendix A, item I. Range: 10-2000 psi Linearity: $\pm 1\%$ full range Sensitivity: 2.5 mv/psi Overload: Maximum pressure, 500 psi Natural frequency: 1.5 mc Resistance: 10^{10} min."

have been developed which utilize the principle of the traveling wave to improve the high-frequency response. (Small-interval reflections occur from the termination of the traveling-wave structure, but these are resolvable.)

The response of such a gage is shown in figure 11. The first photograph shows the leading edge of a shock wave generated in the 4-inch shock tube using a very fast oscilloscope sweep speed, 1 μ sec/cm; figure 11a shows the gage output fed directly into an oscilloscope having a rise time of less than 10 nanoseconds. The second photograph, figure 11b, shows the signal filtered by the charge amplifier (cathode follower, bandwidth 100 kc) with a rise time of 3 microseconds. The third photograph, figure 11c, is a complete, reflected pulse display of this gage at a much slower sweep speed, 2 milliseconds per centimeter. The arrangement of the shock tube for conducting such a test is shown in figure 9. The signals are fed directly into an oscilloscope, or into a system as shown by figure 6.

Two piezoelectric gages having nearly the same response characteristics, and which have just been calibrated, are at positions C and D in the 4-inch tube, figure 9. These gages are connected to the oscilloscopes through cathode followers where both channels have the same gain setting. The pulse-type, pressure/time pictures in figure 12 show the reflected pressure (head-on, position D), figure 12a; and the actual pressure (side-on, position C), figure 12b.

The use of two gages provides a cross-check on the reflected pressure. The reflected pressure taken at positions C and D should be identical. The ratio $\frac{P_2 - P_0}{P_1 - P_0}$ can be obtained directly



Sweep: 1 $\mu\text{sec}/\text{cm}$
 Amplifier bandwidth: $\approx 18 \text{ mc}$
 Rise time: $\approx 0.4 \mu\text{sec}$
 Displacement: 0.05 v/cm,
 reflected
 pressure

a. Gage coupled directly to Tek. 551 scope



Sweep: 20 $\mu\text{sec}/\text{cm}$
 Cathode-follower bandwidth: $\approx 100 \text{ kc}$
 Rise time: 3 μsec
 Displacement: 0.02 mv/cm,
 reflected
 pressure

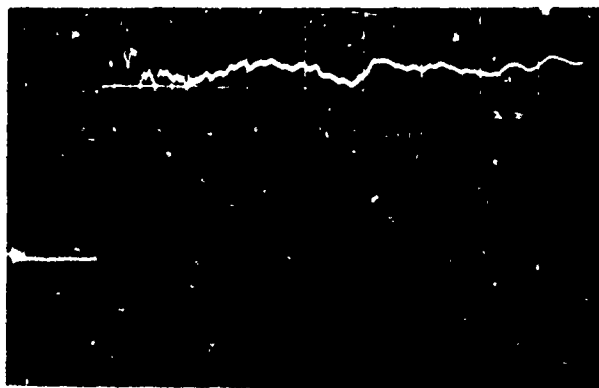
b. Gage coupled first to cathode follower, then to Tek. 551 scope



Sweep: 2 msec/cm
 Cathode-follower bandwidth: $\approx 100 \text{ kc}$
 Rise time: 3 μsec
 Displacement: 0.02 v/cm,
 reflected
 pressure

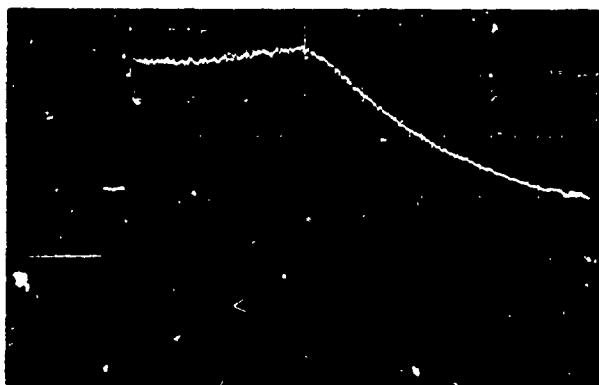
c. Gage coupled simultaneously to cathode follower, Tek. 551 scope

Figure 11. Photographs of 4-inch-shock-tube reflected-pressure pulses for an ST-4 tourmaline gage (traveling-wave principle) which is threaded directly into the steel wall of the shock tube



Gage: ST-2
 Sensor: Lead metaniobate
 Sweep: 20 μ sec/cm
 Displacement: 0.5 v/cm
 Rise time: 5 μ sec (cathode
 follower ac-coupled
 to Tek. 551 scope)
 (Gage threaded loosely in end
 plate of shock tube.)

a. Reflected pressure of gage in closed end of 4-inch shock tube



Gage: ST-2
 Sensor: Lead metaniobate
 Sweep: 2 msec/cm
 Displacement: 0.5 v/cm
 Rise time: 5 μ sec (cathode
 follower ac-coupled
 to Tek. 551 scope)
 (Gage threaded directly into
 side wall of shock tube, four
 inches from reflecting end
 plate.)

b. Side-on pressure of gage in closed end of 4-inch shock tube

Figure 12. Photographs of reflected and side-on pressures of gages in, and near, closed end of 4-inch shock tube

from the single record taken at position C, figure 9. Using equation 9, P_1/P_0 can be computed, from which P_1 is determined. Having made velocity measurements, P_1 is then computed from equation 8. Under controlled conditions, and taking a range of readings, the values of P_1 determined by the velocity and reflected-pressure methods are usually within 2 to 5 percent of each other. The disadvantages of the reflected-pressure method are as follows:

- (1) Reflected-pressure readings can be in error due to overshoot appearing at the start of the pulse which may be interpreted as data. (This can be avoided by using an essentially nonovershooting gage with a low-pass filter.)
- (2) For reliability, two gages are required: one reading side-on pressure and the other, head-on pressure.
- (3) Nearly complete isolation from cross-axis pick-up is required.

c. Pressure-tank method.

Because of its many advantages, the pressure-tank calibration method has replaced the velocity and reflected-pressure methods. This calibration method is preferred because of its simplicity, increased pressure range, portability, improved accuracy, ease of operation, and excellent calibration repeatability.

Basically the tank calibrator consists of a small, light tank capable of withstanding pressures as high as 400 psi, and a quick-acting solenoid valve. One of the possible assemblies of a pressure-tank calibrator is shown in figure 13.

The solenoid is actuated by closing the switch to the portable 45-volt battery supply. This opens the air pressure valve and places the tank pressure on the piezoelectric gage. A family

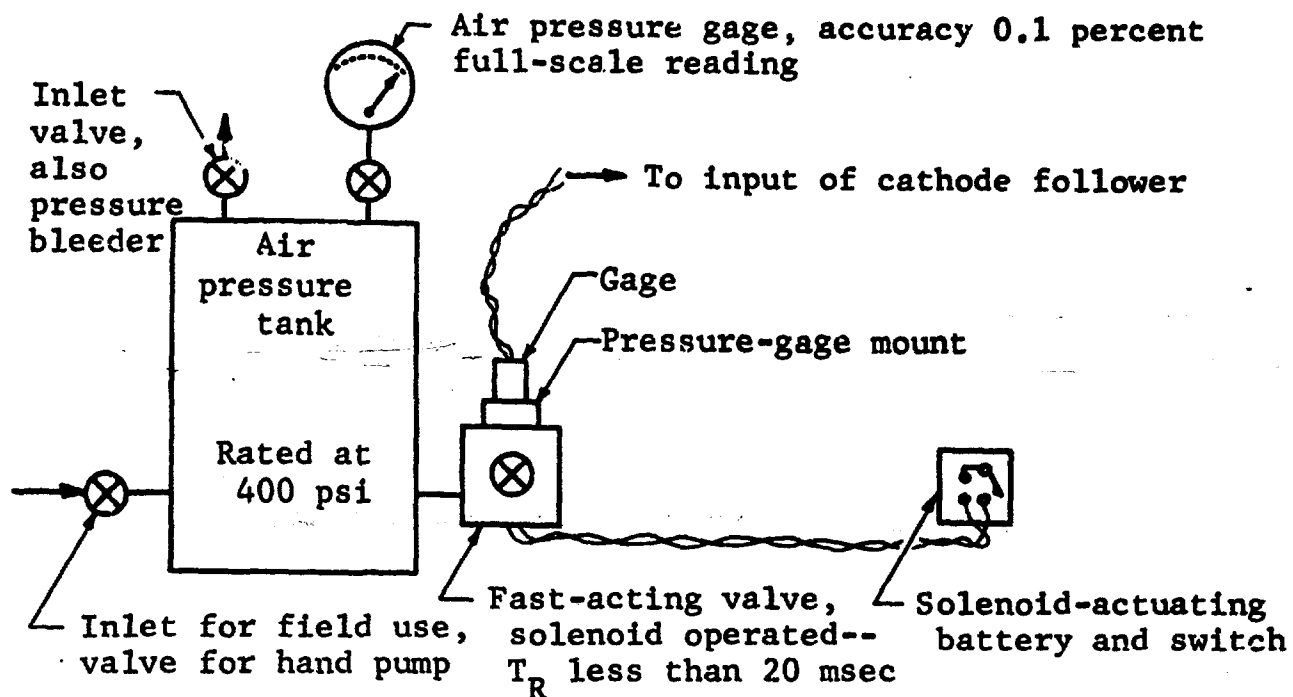


Figure 13. Diagram showing details of portable, pressure-tank calibrator



Sweep: 20 msec/cm
Displacement: 1 v/cm

Figure 14.. Photograph of family of pressure curves vs. displacement curves obtained with pressure-tank calibrator, 0 to 70 psi, in 10-psi steps

of calibration pulses is shown for a piezoelectric gage in figure 14 for a range of pressures. The rise time, T_R , of the pulses varies from 2 to 20 msec depending upon the speed with which the solenoid responds. The dc portion of the pulse, which remains essentially flat (less than 0.1 percent droop in 50 msec), is used for the calibration. Here the droop in the flat portion of the pulse depends upon the pressure-gage design and associated circuitry and not upon the pressure tank. The pressure drop in the tank, due to actuating the solenoid, is insignificant.

Using a precision, air pressure gage (accuracy 0.1 percent of full-scale reading), plots of displacement versus pressure (oscilloscope displacement can be converted to volts/psi for a known, total, circuit capacitance, C_1 , or to pQ/psi) for most gages can be made from 0 to 300 psi with essentially no deviation from a linear plot. Excellent repeatability is possible where the temperature is constant; consequently, it is important that the sensor be shielded from temperature gradients. The shield can be a thin cover over the gage, which has low thermal conductivity. The thermal time constant is usually long enough to allow the pulse information to be recorded before the thermal effects appear on the record. Typical plots of the output of a piezoelectric gage (mv/psi) held at 22° C., 47° C., and 63° C. are shown in figure 15. These plots clearly show the change in output due to temperature, but the linearity is not affected when the gage is maintained at a constant temperature.

The next section describes a short-time calibration technique which eliminates the need for maintaining a history of gage-calibration plots, for checking aging effects, etc.

d. Short-time calibration technique.

The short-time calibration method is not a new method in establishing the accuracy and reliability of measurements. Briefly:

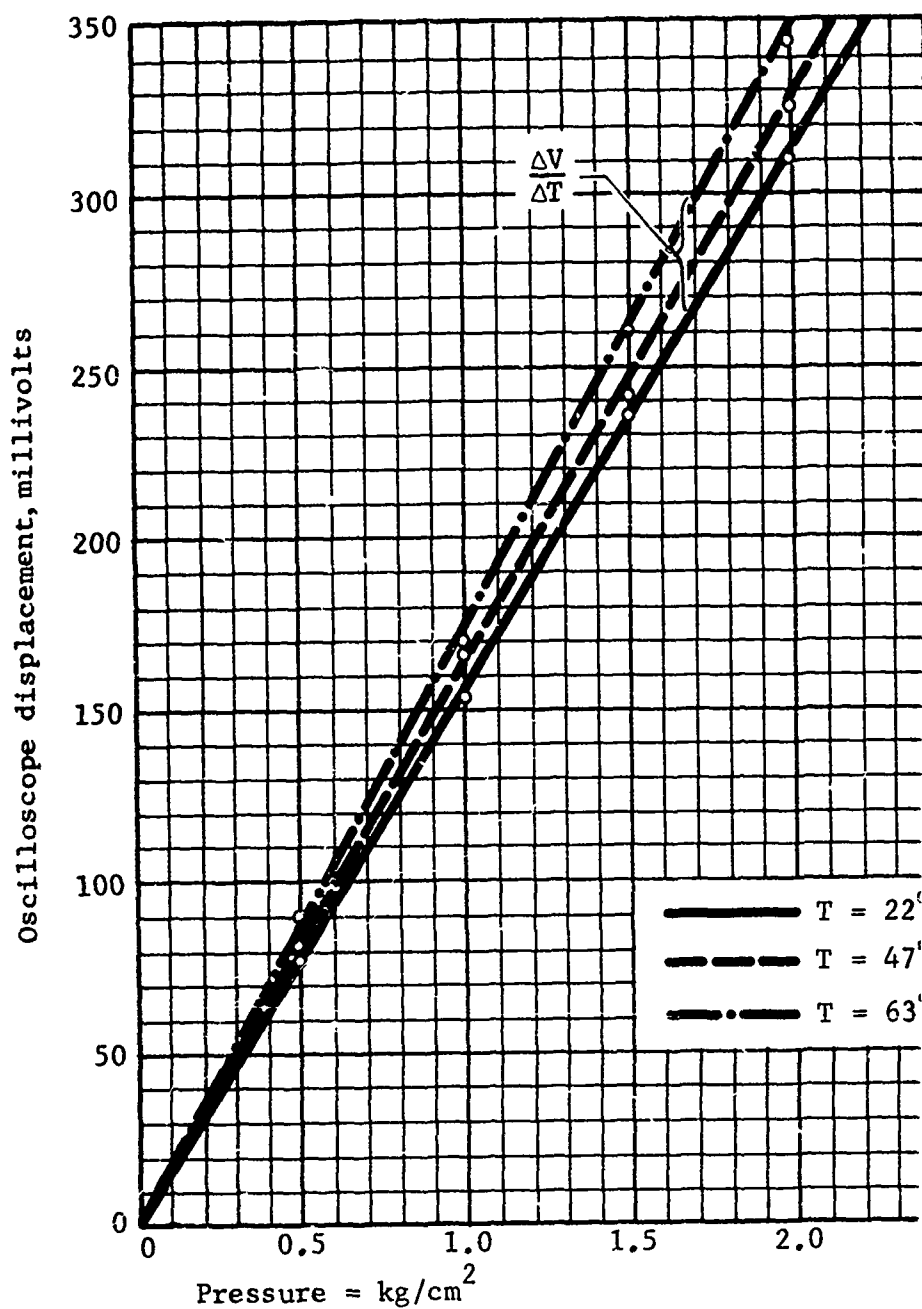


Figure 15. Graph showing piezoelectric gage output vs. ter (ST-2)

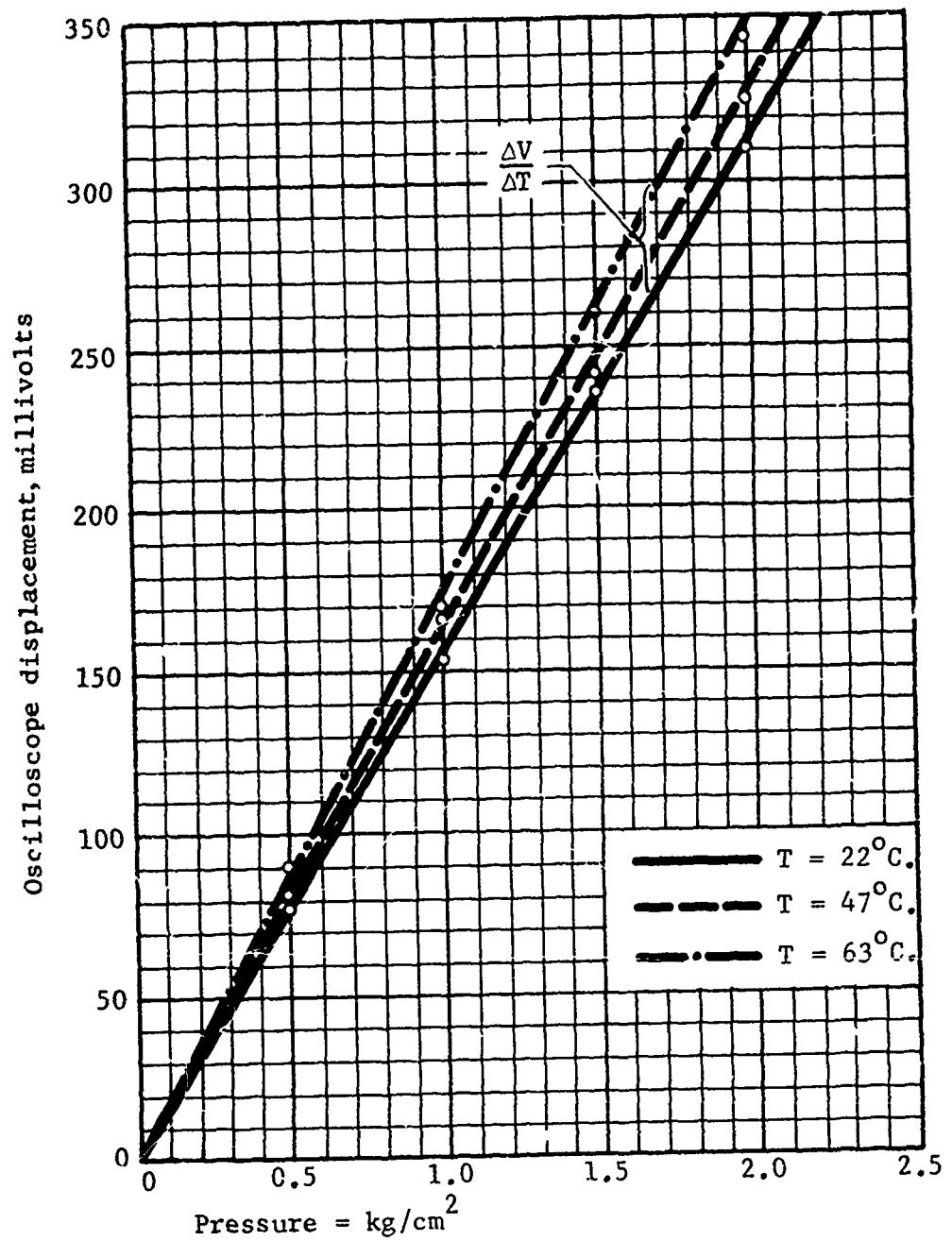


Figure 15. Graph showing piezoelectric gage output vs. temperature (ST-2)

the method is to calibrate the gage just prior to, and after, the shock wave which is to be measured. Here the time interval is as short as possible commensurate with the test conducted. It is assumed that the changes in all the variables (gage, amplifiers, etc.) which can influence the measurements of a test are essentially constant in a short time interval.*

The pressure-tank calibrator being portable can be easily carried to a pressure-sensing station which allows a complete system calibration (gage, amplifiers, and recorder) just prior to, and after, the generation of the shock wave. The pressure gage can be transferred rapidly from its sensing position (with the exception of buried gages, etc.) to the gage mount on the pressure-tank solenoid, and a range of pressure pulses can be applied to the sensor, figure 10. These pulses can be observed on the oscilloscope, photographed, as shown in figure 14, and used as a calibration record.

The plots are recorded directly in voltage versus psi and do not require any further conversions. The gain of the system is adjusted so as to record the maximum pressure without blocking.

If required, calibration data can be obtained for a permanent record by placing them on tape, paper or film. For example, the same data shown in figure 14 can be recorded on tape as depicted in figure 16 where the calibration pulses are shown in time sequence. Comparison of the calibration data prior to and after the shock wave shows the changes in gage performance which have occurred during the short-time interval.

Precise calibration voltages can only be coupled into the recording portion of the entire system and can be placed on the tape

*"Short time" is used here only in a comparative sense.

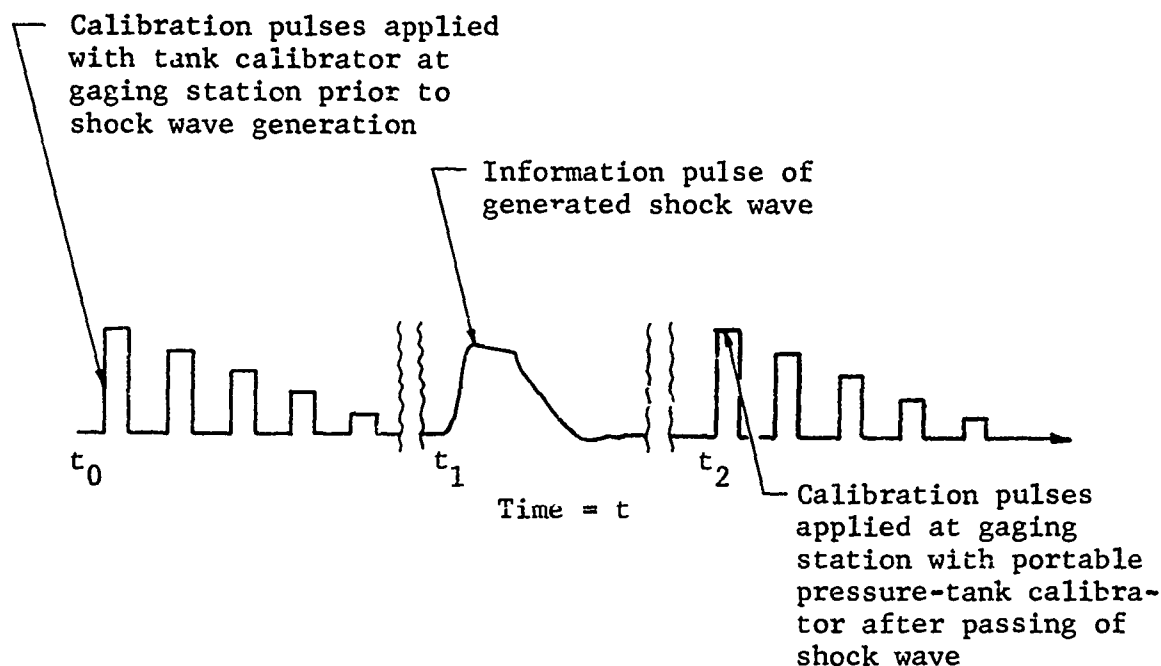
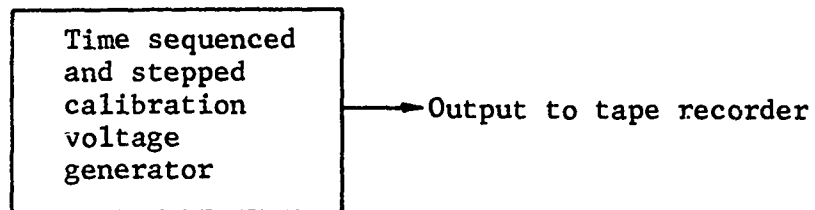


Figure 16. Diagram of tape recording of calibration pulses applied to the piezoelectric-type gages at gaging stations by short-time calibration method

prior to and after the test, figure 17. Such calibrations serve to show the performance and stability of the tape recorder, but they do not provide a complete check of the system. Whenever possible, system calibrations should be used since they eliminate any doubt about the performance of any step of the cascade.

If the gages used are definitely known to be linear, then it is necessary to record only one pressure for calibration purposes, figure 17b. But this procedure is not recommended unless the gage characteristics (as a function of temperature, etc.) and performance history are well known.

For most tests the time, $t_2 - t_0$, figure 16, can be reduced to 10 minutes; however, it usually takes about 30 minutes. Experiments show that under closely controlled test conditions the



- a. Calibration voltages applied to tape recorder without going through entire system



Sweep: 200 msec/cm

- b. Example of single calibration pulse

Figure 17. Diagram showing calibration voltages applied to tape recorder, and photograph of single calibration pulse

change in the calibration data for the piezoelectric gage for $t_2 - t_0$ is seldom discernible.

4. SOURCE AND CAUSE OF ERRORS.

a. Pressure measurements in air and soils.

The previous discussion dealt with the measurement of air shock-wave pressures $P(t)$ whose positive-phase durations were of the order of 10 to 200 msec, where $P(t)$ was transformed to an electrical pulse. The discussion is now extended, briefly, to the shock-wave pressure pulse as it propagates into denser media such as soils. The air shock wave undergoes a change as it enters the more dense medium. A comparison of the electrically transduced air shock pressure wave and the pressure wave in the soils follows:

The pressure pulse (air shock wave) rises in much less than a microsecond. It generally maintains a flat top for approximately 1 to 10 msec, decays to zero overpressure in 10 to 200 msec, and is then usually followed by a negative pressure phase. The fast-rising pulse appears as an impulse to the gages, exciting nearly all of them into resonance. This is evidenced at the beginning of the recorded pulse data by a damped oscillation which modulates the true pulse; the oscillation amplitudes may be as great as 100 percent of the true signal amplitude. This extraneous signal is damped in approximately 0.2 to 5 msec, depending on the gage and sensor construction. This modulation component can be filtered out with a low-pass filter with f_h (high-frequency, 3-db cutoff) around 30 kc.

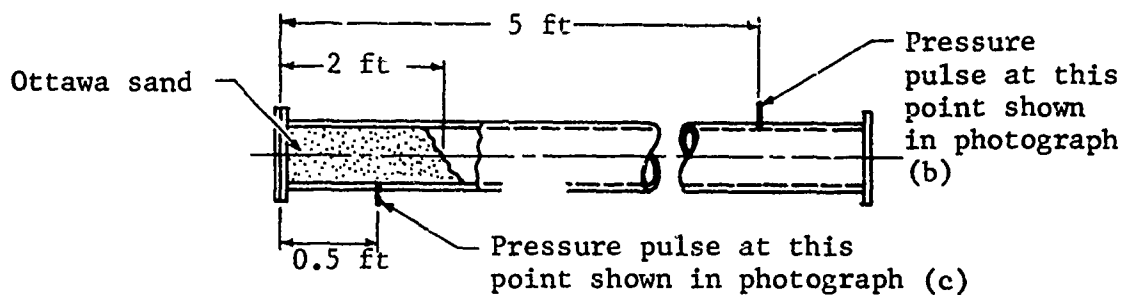
As the shock wave goes from air to a much denser medium, the shock-wave pulse is modified due to the sonic-propagation properties of the medium. (This phenomenon has an electrical counterpart in the transfer function where a loss factor is included and may be thought of as a lossy acoustic filter.) The phenomenon is evidenced by the retarding of the rise of the pulse (slower rise time) and the stretching of the pulse. For the electrical system, this is analogous to the output of a narrow-band system to a square pulse input. This effect is clearly shown in photographs of an air

shock pulse (taken in the 4-inch tube with the end closed) and the same pulse taken in Ottawa sand, figure 18. Except at the air/soil boundary, where reflected pressure is encountered, the maximum amplitude of the pulse decreases due to the attenuation and transfer properties of the soil. Durelli¹⁴ shows the changes in the transduced pulse of the shock wave as it passes from the air to the air/soil boundary, and then to the soil by a sequence of properly positioned gages which register the phenomena.

b. Errors introduced by the equipment.

The pressure pulses for air and soil, when transformed by the piezoelectric gage to charge variations, require different characteristics for their associated electronic systems; i.e., cathode follower, amplifiers, and recording units (oscilloscope, oscillogram, and tape). Both systems require a charge amplifier (cathode follower) to prevent charge leakage at the input of the system. (Poor insulation resistance in this circuit can introduce considerable leakage which seriously modifies the true pulse-time history. Maintaining a high, leakage resistance in this circuit is very important.)

The overall bandwidth of the system, which includes the gage, must be adequate to reproduce accurately the actual pressure pulse. Both the air and soil gage require a very low frequency response to follow accurately the slow, varying portion of the shock wave, preferably dc. The low-frequency response of most ac-coupled systems is inadequate to maintain the error within 5 percent. An ideal, low-response condition is to have a direct-coupled system throughout; however, dc-coupled systems are subject to drift problems. Short-time techniques can largely overcome this objectionable feature, especially when, just prior to the generation of a shock wave, the dc level is returned to its reference position. (This can be accomplished for all gages simultaneously by a master



a. Sketch of Ottawa sand pressure pulses



Gage: ST-2
 Sensor: lead metaniobate
 Sweep: 5 msec/cm
 Displacement: 0.5 v/cm
 Rise time: 5 msec (cathode
 follower ac-coupled
 to Tek. 551 scope)

b. Gage placed in side-on position just ahead of sand-filled end of shock tube



Gage: ST-2
 Sensor: lead metaniobate
 Sweep: 5 msec/cm
 Displacement: 0.5 v/cm
 Rise time: 2 msec (cathode
 follower ac-coupled
 to Tek. 551 scope)

c. Gage placed in wall of shock tube in side-on position in sand-filled end of shock tube

Figure 18. Photographs of pressure pulse in closed-end, 4-inch shock tube, with gages placed in side-on position (b) ahead of and (c) within sand-filled end of shock tube, and sketch of pressure pulses

control switch.)

For the measurement of the air shock wave, the leading edge of the pressure pulse requires an amplifier high-frequency cutoff (3 db) in excess of 150 kc. Using equation 4, T_{R_1} (for the amplifier alone), becomes approximately 2.5 μ sec. The rise time of a well-designed piezoelectric gage for head-on pressure measurements is around 5 μ sec. Thus from equation 5, the total rise time of gage and amplifier may be approximated, $T_R \approx [(5)^2 + (2.5)^2]^{1/2} \approx 5.5$ μ sec. A system having an overall rise time of this order will not appreciably modify the high-frequency portion of the pulse. The amount of this error in relation to rise time and bandwidth is analyzed in the following section. The low response is usually no problem since equipments are available whose low-frequency response characteristics introduce very little distortion.*

c. Fast-rise aspects of pressure pulses.

The most critical measurements are those for air shock-wave overpressures in which the rise time of the pressure pulse is less than a fraction of a microsecond. To reproduce faithfully the initial rise of the pulse requires a very fast responding gage, usually piezoelectric types, and a nonovershooting, amplifying system which does not affect the high-frequency components of the electrically transduced shock wave pulse.

Some of these effects can be clearly shown by an example. A piezoelectric gage is used which has a slow rise time of 50 μ sec;

*Where the low- and high-frequency components are well known, individual amplifiers can be used to cover these two ranges. Emphasis and deemphasis are used to compensate for the system gain versus the frequency variations.

this gage is used in conjunction with the recording system shown in figure 19.

Figure 20 depicts the pulse deterioration as it progresses through the system. An air shock pressure wave, which has a fast rise and a rapid exponential decay, is purposely considered since it aids in showing these effects. A pressure wave in soils is subject to the same bandwidth effects, but they are usually very small and can be disregarded.

Trace A, figure 20, is the fast-decaying, pressure/time history generated by detonating primacord in the 2-foot vertical tube. Because of the inadequate high-frequency response of the transducer (which can be thought of as the time the shock wave takes to traverse the gage face), the leading edge of the pulse is changed. Instead of detecting Trace A as shown in figure 20, a modified pulse is recorded as Trace B or C. The severity of this pulse change is readily apparent when the expanded sweep of the front part of the pulse is observed. Actually, what is observed for the overpressure, ΔP , for a slow-responding gage is ΔP_1 for Trace B, and ΔP_2 for Trace C. Thus, for fast-decaying pressure pulses, the calibration of the gage, when using the pressure-tank method represented by the dc-calibration level (fig. 20), would be in error. The amount of error is given by

$$\text{percentage of error} = \frac{\Delta P - \Delta P_1}{\Delta P} \times 100 \quad (10)$$

It is thus seen that ΔP is really represented by ΔP_1 or ΔP_2 , depending on two different gage characteristics. In contrast, shock pressure fronts that have a considerable flat-top region, figure 21, eliminate the problem of not being able to calibrate on the short-interval, dc level (actual pressure) indicated in figure 20.

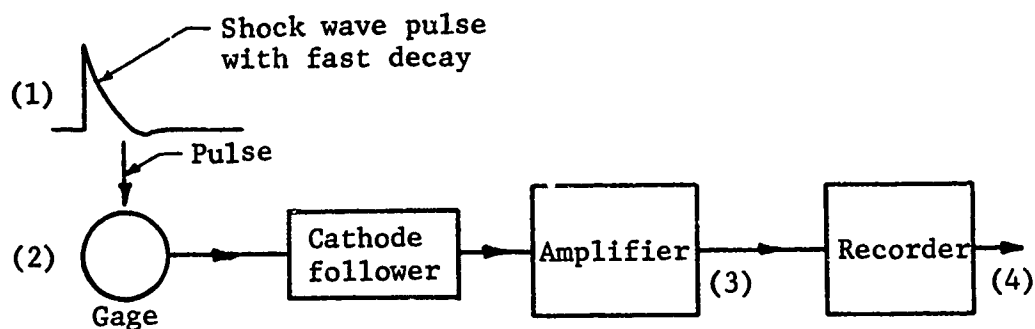


Figure 19. Diagram of pressure-pulse distortion due to gage and recording system in 2-foot vertical shock tube

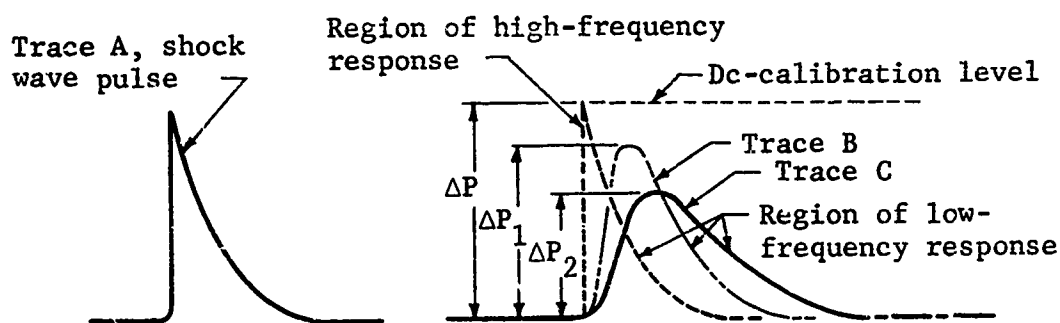


Figure 20. Diagram of pressure-pulse change due to response function of gage and recording system (2-foot vertical shock tube)

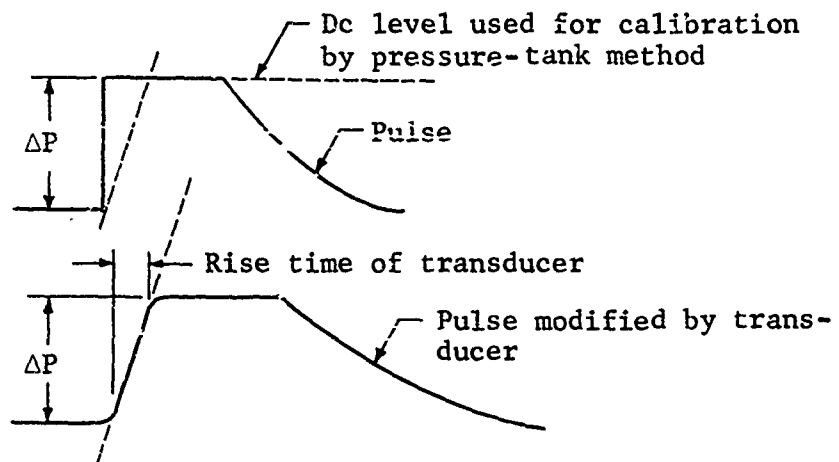


Figure 21. Errors encountered in calibrating fast-decaying pressure pulses when using pressure-tank method of calibration

Figure 21 shows the elimination of this change of amplitude when the dc level is greater than 1 msec; the gage output rises to the proper pressure level before the pulse decays. Although this is not a frequent situation, care should be exercised in accepting the tank calibration in conjunction with fast-rising and decaying-pressure pulses, especially if a slow-responding gage is used in conjunction with an inadequate system bandwidth.

d. Errors introduced by noise sources.

As shown in figure 6, noise can be introduced into every stage of the system (amplifiers, ecc.) which includes the piezo-electric gage, its mount, and its location in the shock tube. The type of noise, its amplitude and phase, and its coupling into the system are quite varied.

Before it is possible to analyze the noise effects on the recorded data, it is necessary to define the meaning of noise as it applies to the various gages used for measuring stress. Consequently, for this report, noise (N) is defined as any extraneous

or undesirable signal which modulates or modifies the true information signal (S). The signal-to-noise ratio (S/N) is used in the usual sense to evaluate the performance of the system. For example, if the noise components associated with a gage output are low, $S/N \gg 1$, they are usually ignored in most data analyses. This definition is also applicable to strain, velocity, displacement, acceleration, and other similar measurements encountered in shock-tube tests.

In conjunction with the signal-to-noise information, the question of how effectively a high signal-to-noise condition is utilized depends upon the resolution of the recorded data. This condition is usually exemplified by having available a high signal-to-noise input where the resulting photographed output of the oscilloscope trace, or oscillograph recording, of the stress information exhibits poor resolution due to inadequate film contrast, overbloom of the trace spot, etc. The resolution problem can be circumvented by tape recorders or digital readout systems; however, such equipments are not feasible nor readily available for most tests.

(1) Noise sources.

The following noise sources, which are to be reviewed fit the given definition for noise. Each of these sources is discussed mainly in relation to the piezoelectric stress gages, with the emphasis being placed on the degradation of the information signal (S). Methods by which the noise source, or its effects, can be reduced or eliminated are presented.

(a) Natural and resonant frequencies.

A gage has certain resonant characteristics which are excited only under certain conditions; furthermore, resonance is specified along a particular excitation axis (there

can be actually five degrees of excitation: three orthogonal, two rotational). A gage is specified for operation in the desired sensing direction. However, resonance may be excited along a preferred axis or axes.

This excitation is an extraneous signal which modulates the true pressure pulse. A more exact terminology, given by the American Standards Association⁵ in conjunction with these excitations, follows:

1. Undamped natural frequency: Regardless of the damping present, the undamped natural frequency of a linear pickup (linear response) having a single degree of freedom is the frequency of sinusoidal excitation at which the motion of the mass element lags behind the motion of the housing of the pickup by a phase angle of 90 degrees. For more than 1 degree of freedom there may be many frequencies where this condition is met. The lowest of these frequencies is taken as the undamped natural frequency.
2. Damped natural frequency: The damped natural frequency of a linear pickup is the frequency of its damped free vibration when the pickup housing is held fixed. In pickups having several degrees of freedom, there may be as many damped natural frequencies as there are degrees of freedom.
3. Resonant frequency: The resonant frequency is defined only for linear pickups with a damping ratio of less than 0.707. The resonant frequency is the frequency at which the sensitivity of the pickup is a maximum. Additional resonances corresponding to modes in which the principal displacements occur locally in the spring, housing, or attached fittings are sometimes excited, particularly by shock motion (impulse).

Of particular interest is the damped natural frequency since it is the one usually excited by a shock wave. This

damped natural frequency can be as low as 30 kc for diaphragm-type gages¹⁵ and as high as 1.5 mc for traveling-wave-type gages. Lower order mode resonances occur due to improper design of the mount, lack of acoustical filters, and inadequate isolation of the sensor for cross-axis pickup.

The damped natural frequency can be easily demonstrated by applying an impulse to the gage. The piezoelectric gage is placed on the end plate of a laboratory shock tube so as to be in a head-on position as shown in figure 9, and it is excited into its damped natural frequency by a shock wave of sufficient strength. This excitation is truly an impulse. Similar effects can be achieved by rapidly striking the sensor with a hard object, etc.

The damped natural frequency appears as a modulation on the leading edge of the recorded, electrically transduced pressure pulse, figure 2. The amplitude of the first cycle of this damped frequency is a function of the strength of the impulse and is usually found to be positive going. A photograph of this modulating component (noise) is shown in figure 3 for a diaphragm-type gage.

Six photographs of this modulating component (noise) are shown in figures 22 and 23 for six piezoelectric gages which differ in design and sensor material. The materials are barium titanate, lead zirconate titanate (PZT-5), lead metaniobate, tourmaline, Piezite (trade name), and quartz, respectively. These gages were all excited by step-function pressure pulses.

The first gage, figure 22a, uses the earlier type barium titanate ceramic which is in the form of a 1/8-inch-diameter cylinder, 1/8 inch long; the mount includes a rubber insert to provide cross-axis isolation. (See appendix A for pictures of this and the following gages.)



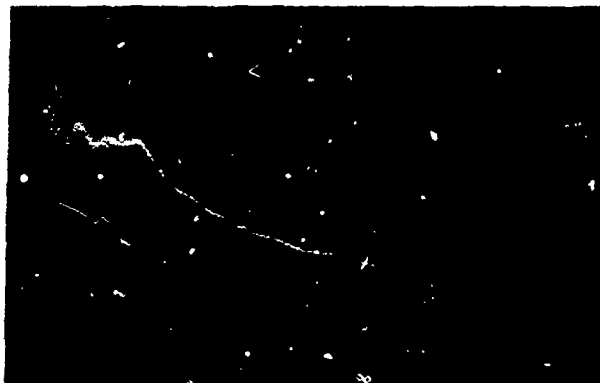
Gage: early-type barium titanate
 Sensor: old-type barium titanate, circular cylinder
 Sweep: $\mu\text{sec/cm}$
 Resonance: $\approx 330 \text{ kc}$
 Rise time: $4 \mu\text{sec}$ (in end plate of 4-inch shock tube, 35-psi reflected pressure; filtered by cathode follower, 100 kc)

a. Photograph of the resonance effects of one of the early developed gages using a barium titanate sensor



Gage: Piezite
 Sensor: modified lead zirconate titanate, diaphragm
 Sweep: $100 \mu\text{sec/cm}$
 Resonance: two modes, 6 and 100 kc
 Rise time: $\approx 5 \mu\text{sec}$ (side-on position, rings in side-on position; gage ac-coupled directly to oscilloscope)

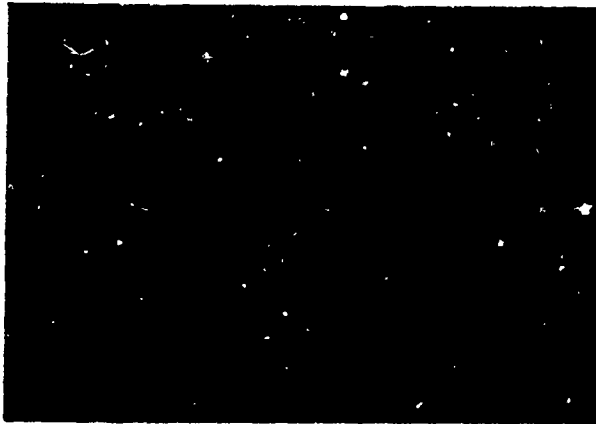
b. Photograph of the resonance effects of a piezoelectric gage of the stretched-diaphragm design



Gage: quartz sensor
 Sensor: quartz, stretched diaphragm
 Sweep: 5 msec/cm
 Resonance: $\approx 40 \text{ kc}$
 Rise time: $\approx 10 \mu\text{sec}$ (side-on position, rings in side-on position; gage dc-coupled through cathode follower, 150 kc total bandwidth)

c. Photograph of the resonance effects of a piezoelectric (quartz) gage of the stretched-diaphragm design

Figure 22. Photographs of resonance tests of piezoelectric pressure gages by impulse method



Gages: PZT-4 and PZT-5
 Sensor: PZT-4 and -5, lead zirconate titanate
 Sweep: 20 μ sec/cm
 Resonance: two modes, \approx 33 and \approx 125 kc
 Rise time: 8 μ sec (in end plate of 4-inch shock tube, 35-psi reflected pressure)

a. Photograph of the resonance effects of a gage similar in design to figure 22a but with improved sensors



Gage: tourmaline sensor
 Sensor: tourmaline, traveling-wave principle
 Sweep: 1 μ sec/cm
 Resonance: \approx 1.5 mc
 Rise time: 0.4 μ sec (in end plate of 4-inch shock tube, 35-psi reflected pressure)

b. Photograph of the resonance effects of a gage using the traveling-wave principle



Gage: lead metaniobate sensor
 Sensor: lead metaniobate, flat wafer, 1/8-inch diameter
 Sweep: 20 μ sec/cm
 Resonance: \approx 250 kc
 Rise time: 2 μ sec (in end plate of 4-inch shock tube, 35-psi reflected pressure)

c. Photograph of the resonance effects of a gage designed for moderately fast response (200 kc)

Figure 23. Photographs of resonance tests of piezoelectric pressure gages by impulse method

The gages shown in figure 22b and c use piezoelectric-type sensors and a stretched diaphragm over the sensors. Resonance for such gages occurs at a much lower frequency, under 40 kc.¹⁵ A filter is usually required to remove the resonance component.

The gage in figure 23a uses the same size and shape sensor as in figure 22a, except that the sensor material is either PZT-4 or PZT-5, Clevite.^{1,2,4} The use of a more rigid mount (no isolation) accounts for the higher cross-axis pickup and the corresponding lower resonant frequency.

The gage in figure 23b utilizes tourmaline as the sensor in a traveling-wave principle. The resonant frequency is slightly over 1.5 mc; however, the output of the tourmaline sensor is about 1/10 to 1/20 that of the barium-titanate-type sensors.

The gage in figure 23c has a small, 1/8-inch diameter, lead metaniobate, wafer-type sensor, air isolated, and with an acoustical filter. The resonance frequency is slightly over 250 kc.

All of these gages were subjected to the same impulse. The sweep speeds are generally different in order to show the resonant effects for different resolutions in time. Resonance effects are generally obscured with slow sweep speeds.

The amplitude is decreased for some of these oscillations due to the filter action presented by the following amplifiers and recorders. The pulse in figure 23b is different in that it is not filtered; it shows the damped natural frequency of a piezoelectric gage using the traveling-wave principle which is ac-coupled directly to an oscilloscope having a bandwidth in excess of 15 mc.

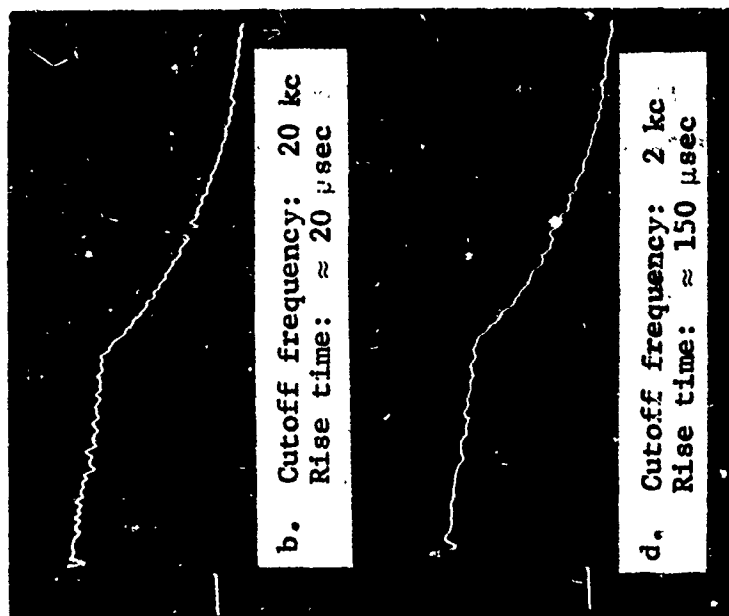
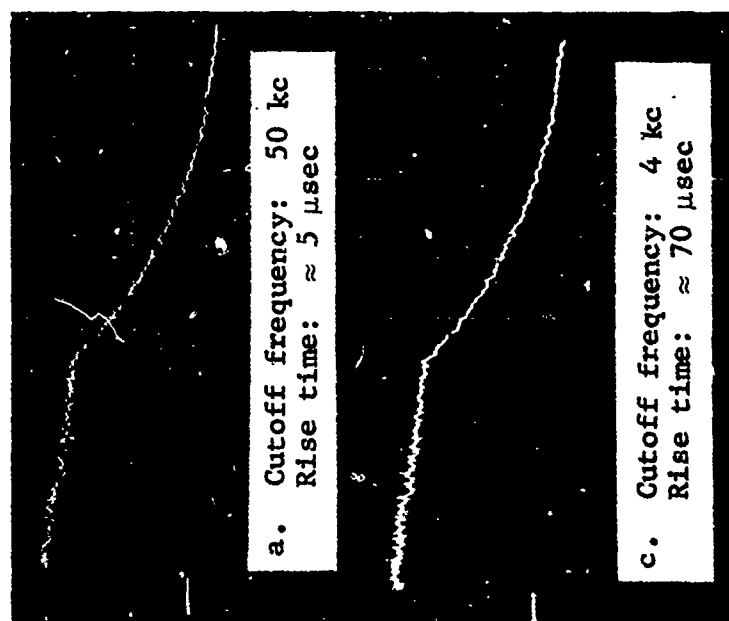
The natural frequency and the damping ratio (C/C_c = damping ratio of a linear, viscously damped, mass-spring system where C is the damping constant of the system, and C_c is the damping constant for which the system is critically damped) of a gage can be measured by subjecting the gage to a sinusoidal exciter. An exciter applies a controlled motion to the mounting surface of a gage. A sinusoidal exciter is capable of applying sinusoidal motion of controllable frequency (0 to approximately 50,000 cps) and amplitude to the housing of the gage. Reference to theoretical response curves, from which two (or more) amplitudes are taken at different frequencies, allows determining the ratio C/C_c .

Both the impulse and exciter methods are used for calibrating accelerometers with piezoelectric-sensing elements to determine the undamped, damped, and resonant frequencies. These methods are presented in the American Standard Methods⁵ and by Bouche.¹⁶

To prevent resonant-type noise from appearing in the data requires operation below resonant conditions (slower rising pulse such as in soils) and the application of filters wherever possible. The effectiveness of a low-pass filter is shown in figure 24 for a typical shock wave using a gage with a resonant frequency of approximately 100 kc. A dual electronic filter is used, with unity overall gain and a rolloff of 36 db per octave. The low-pass band was from 0 to f_h , where f_h was 50, 20, 4, and 2 kc, respectively. The noise components were essentially missing for f_h less than 4 kc, figure 24d. (The electronic filters show some overshoot.)

(b) Cross sensitivity.

A gage is generally designed to have a maximum sensitivity along a particular axis, and with a minimum sensitivity along the other axes. This indicates that three sensors are usually



Gage: ST-2 Sweep: 2 msec/cm Displacement: 0.2 v/cm

Gage output filtered by two low-pass sections of electronic filter (gain unity)

Figure 24. Four-inch shock tube, transduced pressure pulses at output of low-pass filter

required for complete three-dimensional information (rotation excluded). Even with special designs, the cross-axis pickup can be excessive under certain test conditions.

The amount of cross-axis pickup is dependent on the type sensor used (size and shape), the gage design (mechanical and electrical), the degree of isolation possible in mounting the gage to the shock tube (also other appurtenances), and the placement of the gage in either the shock tube or in other media (soils, etc.).

The sensitivity of a particular element such as lead zirconate titanate can be obtained for various shapes from the technical literature, Clevite,^{1,2,4} and the percentage of cross-axis sensitivity can be computed; these are of the order of 2 to 10 percent of the main-axis value. In the mounted position, the relative magnitude of the cross-axis pickup may be as high as 25 percent of the information signal. It is informative to note that in shock-front velocity measurements, a 5 percent cross-axis pickup of the shock-wave amplitude being transmitted down the steel, side wall of the shock tube is high enough in amplitude to actuate a time-interval counter prematurely, whose on/off gages are mounted in the wall.

The six pressure gages used in figures 22 and 23 were all measured for cross-axis pickup where the gages were mounted directly in the wall of the 4-inch shock tube. The first 10-foot section of the 4-inch shock tube in which the gage was mounted was not decoupled by a rubber O-ring. A disturbance of relatively high magnitude was transmitted in the wall of the tube due to the generation of the shock wave. This disturbance was coupled cross axially by the gage and appears as a noise modulation. This is shown for one of the gages in figure 25a where the trace prior to the signal shows the cross-axis pickup of the wave traveling in the steel wall to have a velocity many times greater than



Gage: PZT-5
 Isolator: threaded directly
 into side wall of
 4-inch shock tube
 Sensor: PZT-5
 Sweep: 1 msec/cm
 Displacement: 0.2 v/cm

a. Piezoelectric gage threaded into steel wall of shock tube close to shock-wave generating chamber



Gage: PZT-5
 Isolator: rubber grommet be-
 tween gage housing
 and wall
 Sensor: PZT-5
 Sweep: 1 msec/cm
 Displacement: 0.2 v/cm

b. Piezoelectric gage isolated from steel wall of shock tube by rubber grommet

Figure 25. Photographs of shock waves resulting from piezoelectric gages being threaded into and isolated from steel wall of 4-inch shock tube

the air shock velocity. This noise modulates the pressure signal.

Decoupling the 10-foot section of the 4-inch shock tube at each flange with an O-ring very effectively reduces the steel tube disturbance as is evidenced by figure 25b. It is noted that the trace prior to the actual pressure pulse is entirely free of noise. The modulation seen on top of the pulse can now be attributed to actual pressure variations caused by the gage not being exactly flush with the interior of the tube wall or by the rough surface of the wall itself (causing turbulence).

The same degree of isolation can be achieved by specially mounting the gage from the steel wall. The gage can be isolated by grommets of rubber or nylon (nylon can be easily machined so that it can be threaded in place). The trace prior to the signals in figures 1, 2, and 3 clearly show the amount of cross-axis pickup for gages isolated from the shock-tube wall. Figure 4 shows the cross-axis pickup using one of the gages when it is first mounted in rubber and then in nylon. Both of these materials exhibit good decoupling properties. For some tests, the gages were positioned by external supports and decoupled by a small air gap. The air gap provided the greatest amount of decoupling; however, this installation was applicable only for shock velocity measurements since the pressure leak by the hole in the side wall of the shock tube, centered on the gage, distorted the shock pressure wave.

Another method for determining experimentally the total cross-axis pickup^{*} is to mount the gage directly in the steel wall. Then the pressure sensor is covered with a steel cap which does not contact the main-axis sensor face. The same shock

*Part of the noise component seen is due to the acceleration effects. These components can be separated; however, the overall effects are of real significance.

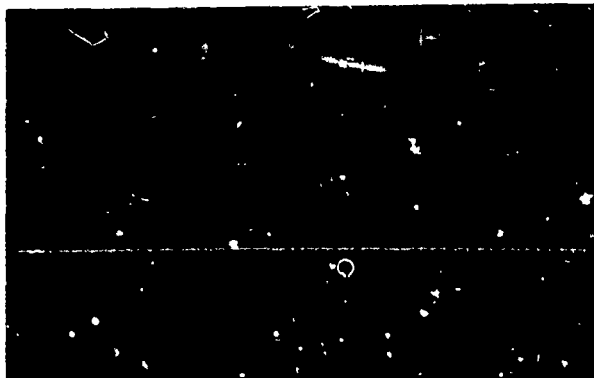
pressure is generated as for figures 2, 3, and 25, and the cross axis history is recorded, figure 26. The first two photographs, figure 26, are for the same gage which has very low cross-axis pickup. For comparison, the pressure-pulse trace on the oscilloscope is, figure 26a, usually 3-cm high for a $\Delta P = 12.5$ psi. The first trace, thus, shows less than 1 percent pickup; the second trace, figure 26b, is for the same overpressure, but the gain has been advanced by ten to provide a better visual comparison. The cross pickup is found to be just perceptible.

Decoupling can sometimes be successfully accomplished by using a short rubber tube to isolate the gage from the steel wall of the shock tube. In the blast section, this method prevents explosion particles from striking the face of the gage which can damage the gage or cause spurious readings. This method has two bad effects: (1) a Venturi effect increases the rise time, and (2) resonance effects can be set up in the inside of the rubber tube. Both of these conditions are demonstrated in figure 26c. The actual pressure pulse ordinarily looks as it does in figure 24a; however, the sweep speed has been reduced by a factor of two.

(c) Mountings.

The mounting of a gage in the side wall of a shock tube is critical. If the gage is not flush with the tube, one can get noise modulation effects which are quite pronounced. This is shown by figure 27 where a gage is (1) recessed 1/8 of an inch, (2) mounted flush, and (3) protruding 1/8 of an inch (reading from top to bottom).

Gages slightly tilted into a head-on position are subject to reflected-pressure effects; this is readily apparent from the model studies. It is sufficient to say here that the placement of gages is very critical and requires a careful analysis for each new gaging problem.



Gage: ST-2

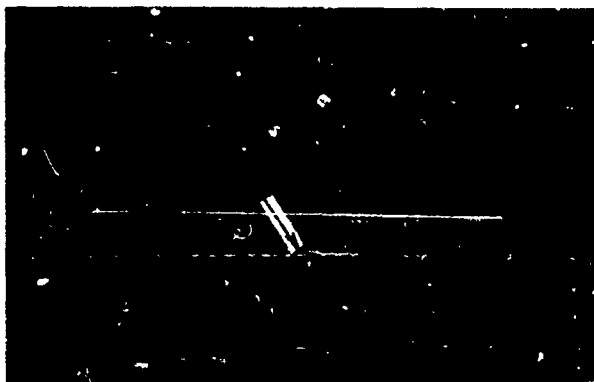
Isolator: threaded directly into shock-tube wall, isolation provided by gage only, side-on mount

Sensor: face capped to prevent pressure transfer

Sweep: 1 msec/cm

Displacement: 0.2 v/cm

a. Photograph of cross-axis sensitivity of piezoelectric gage

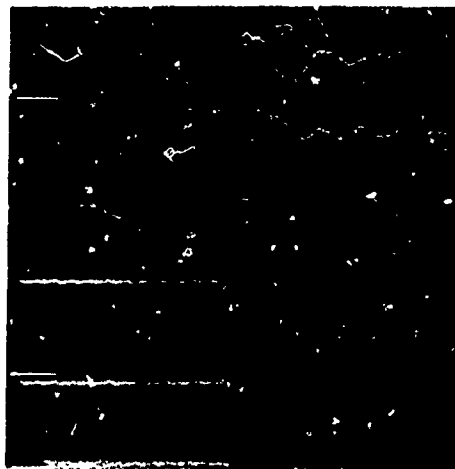


b. Same as (a) except that the amplifier gain is increased by a factor of ten to amplify the slight cross-axis pickup for observation



c. Same as (a) except that the gage is coupled to the 4-inch-shock-tube wall through a 2 1/2-inch-diameter brass tube. Note the Venturi effect, indicated by the increase in rise time, approximately 200 μ sec, and the resonance set up in the tube

Figure 26. Cross-axis sensitivity of piezoelectric gages and decoupling



Gage: ST-2
 Sensor: lead metaniobate
 Sweep: 40 μ sec/cm
 Pressure: $P \approx 12$ psi
 Mounting: upper trace, protruding
 1/8 inch, side-on
 middle trace, flush with
 inside wall, side-on
 lower trace, recessed 1/8
 inch, side-on
 Displacement: upper trace, 0.1 v/cm
 middle trace, 0.1 v/cm
 lower trace, 0.2 v/cm

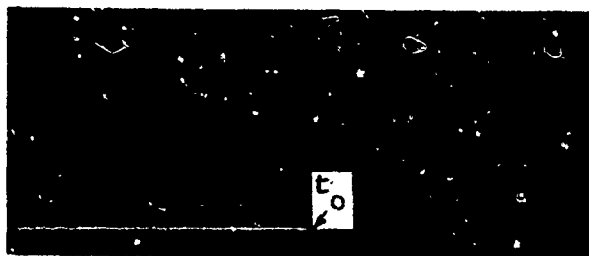
Figure 27. Distortion encountered by not mounting gage flush with wall of 4-inch shock tube (side-on mounting)

(d) Acceleration.

The sensing element of a gage experiences a force due to acceleration. This appears as a noise signal which modulates the information signal. The amount of error this introduces is given in terms of percentage of the full-scale reading per "g" unit.

Experimentally, the acceleration noise can be determined by capping the gage and isolating it as completely as possible and then subjecting it to a known shock pressure. This is done for the main axis, but it can be done for all axes.

This effect is measured experimentally and is shown in figure 28 for a capped gage with the sensing element in a head-on position. The acceleration noise is approximately 5 percent. There are three photographs in figure 28. The complete pressure pulse is first shown for an overpressure of approximately 12 psi. Directly below this pressure pulse is a trace showing the acceleration effects with the gage capped and subjected to the same



Sweep: 1 msec/cm
Displacement: 0.2 v/cm

a. Uncapped gage $\Delta P \approx 12$ psi



Sweep: 1 msec/cm
Displacement: 0.2 v/cm

b. Capped gage $\Delta P \approx 12$ psi



Sweep: 1 msec/cm
Displacement: 0.02 v/cm
(increased by a factor of ten)

c. Capped gage $\Delta P \approx 12$ psi

Figure 28. Photographs of measurement of acceleration noise of a pressure gage

overpressure; the third trace is the same as the second but with the gain increased by a factor of ten to give greater resolution. A cross-axis noise pickup is further removed by gage isolation. If necessary, the acceleration component can be separated by either relative or absolute methods.⁵

(e) Groundloops.

A system groundloop is here designated as any electrical path which allows an unwanted noise current to circulate. This current may appear in the input circuit of an amplifying system and thereby lower the input signal-to-noise ratio S/N. It may also be introduced at any part of the cascade, figure 6. This becomes

a serious problem when the sensor output is low; for example, for small strain or acceleration measurements the gage output signals are quite low and the extraneous noises must be kept to a minimum.

A groundloop may be in some part of the overall system which does not cause any problem; furthermore, the voltage developed by the noise-generating source contained within the loop may be too low in amplitude to be of any consequence. Some ground-loops may be quite extensive and complex but not coupled to driving-noise sources so as to cause a problem. This is why it is extremely important to isolate noise generators (60-cycle neon lights, generators in the equipment, etc.) and to have a good (low-resistance) ground return for the entire system.

A system may contain a number of groundloops and other noise sources (noise voltages coupled into the system by strong magnetic fields) which are difficult to locate and usually more difficult, or impossible, to eliminate. These loops are usually found to be coupled into the system by capacitances that are integral with the system, and cannot be removed by external modifications, or rewiring, of the system. Rather, it requires the redesign of the individual units of the cascade, such as amplifiers, gages, recorders, etc. By redesign, using certain well-known techniques, coupling capacitances can be reduced.

An example of this decoupling technique is shown in figure 29. With a grounded transducer and the capacitances C_1 and C_2 , the primary of the power transformer is coupled into the groundloop, and a current is forced to flow in the input resistance, R (resistance of input cable from gage). By reducing the capacitance C_1 , the current flow can be reduced to an unobjectionable value. This is accomplished by using double-shielded transformers, battery operated amplifiers, etc.

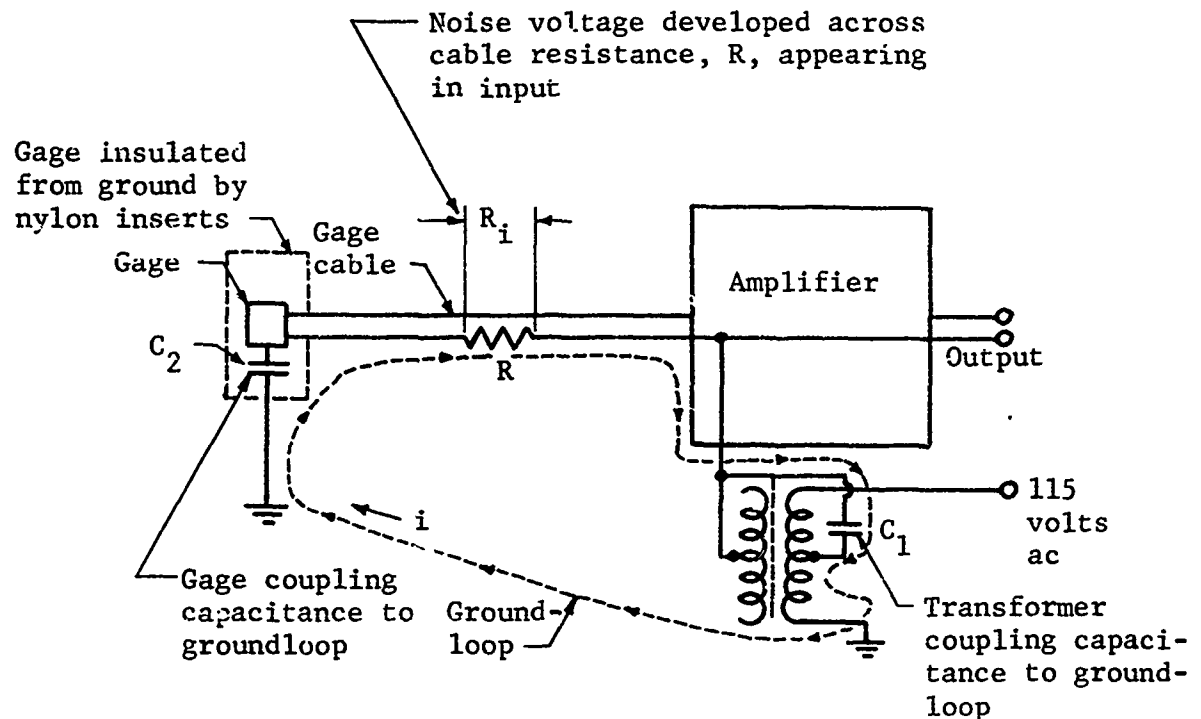


Figure 29. Diagram of typical groundloop found in pressure-measuring system

For most piezoelectric-gage applications, the groundloop can be removed by isolating the gages with insulating mounts which makes the series capacitance to the groundloop negligible.

In some areas, the power-line equipment (transformers, power lines, and motors) induce a strong 60-cycle current into the system. Since this is an easily detected, well-defined, periodic-modulating source, it can be removed from the information signal by certain data-processing methods. When the information is recorded on tape, a differential input amplifier is usually applied to remove the 60-cycle component. For time coherence, one channel of tape is used for recording the noise signal along with the

recording of the data. This method is shown in figure 30 where the original signal with the 60-cycle component is fed into one input of the differential amplifier with an exactly opposing 60-cycle source (both in amplitude and phase) being fed into the other input. The output shows the 60-cycle component removed.

(f) Circuit noise power.

The noise power generated in a stage of amplification (which is sometimes referred to as residual amplifier noise) is usually so low as to be negligible for most applications in conjunction with pressure gages. This may not be the case, however, when one measures very low pressures, accelerations, and strains.

For low-level signals, noise reduction can be achieved by certain refinements in the equipment and the measurement techniques.

The theoretical noise power available over a bandwidth, B , between any two terminals of a passive network when all of its parts are at a temperature, T , is given by the expression

$$N_p = KTB \quad (11)$$

where K = Boltzmann's constant, T = absolute temperature, and B = bandwidth in cycles per second. This expression for N_p can serve as a guide for the minimum noise to be expected in the system. It is important to note that the bandwidth is the only easily controlled factor in this expression; generally temperature cannot be controlled. The use of excessive bandwidth merely introduces more noise into the system. For most pressure gages and their associated amplifiers, this noise level is way below the other noise sources and can be ignored.

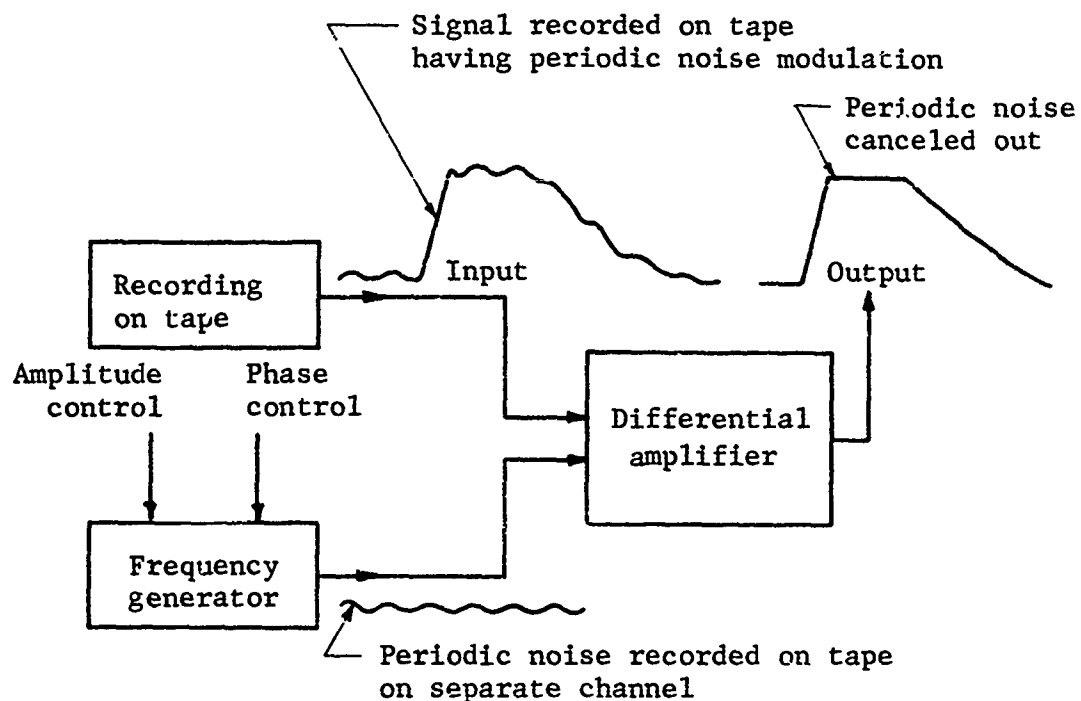


Figure 30. Removal of periodic noise from tape recording

Where low-level signals are encountered, special amplifiers having a low-noise characteristic are required. (The noise level for such amplifiers is of the order of 15 μ volts referred to the input of the amplifier over a frequency range of 0 to 30 kc.) With amplifiers and other equipments in cascade, figure 6, the overall system noise figure, F , indicates that the signal-to-noise is degraded by each unit in the cascade. (The noise figure, F , is defined as $\frac{S_i/N_i}{S_o/N_o}$ where the subscripts i and o represent input and output, respectively. F is generally around 5 to 15 db; for the ideal case, $F = 1$.)

For a cascade of amplifiers such as are required for raising the weak signal up to the level to drive a tape recorder (gains ranging from 10 to 1,000), the overall noise figure,

$F_{1,n}$, is given by the expression

$$F_{1,n} = F_1 + \frac{(F_2 - 1)}{G_1} + \frac{(F_3 - 1)}{G_{1,2}} + \dots + \frac{(F_n - 1)}{G_{1,n-2}} + \frac{(F_n - 1)}{G_{1,n-2}} \quad (12)$$

where F_1 is the noise figure of the first stage, etc., and where $G_{1,n}$ denotes the available gain of the first through the nth stage ($G_1, G_2 \dots G_n$), see figure 6. The important information imparted by this expression is that it is seldom necessary to consider the noise figure of more than two stages of the cascade when the gains G_1 and G_2 are quite large. However, this is not the case for the cascade shown in figure 6 where the gain of the cathode follower (which is required with a piezoelectric gage) is usually less than 0.9. Implicit in equation 12 is the assumption that the bandwidths are equal to each other. It is well to keep in mind that the overall system bandwidth is less than the narrowest bandwidth of any unit in the cascade, and that the overall system rise time is greater than the stage rise time. A more complete analysis can be made of the entire system where the bandwidth of each unit in the cascade is considered, figure 6. The expression for $F_{1,n}$ which includes the bandwidth effects is given by Goldberg.¹⁷

Except for particular low-level applications, the main sources of noise are given by the previous items. The magnitudes of these noise sources are usually much larger than those developed by the amplifiers, recorders, and other equipments.

(g) Temperature variations.

Noise in this discussion applies to a change in the output of the various sensors, in particular the piezoelectric types, due to both rapid and slow temperature variations. The output of the piezoelectric-type sensors, such as lead zirconate titanate (PZT) and lead metaniobate ceramics, is essentially constant as a function of temperature over a certain range of temperature below the Curie temperature, figure 31.

For a piezoelectric gage mounted in the wall of a shock tube where hot gases pass over the gage face, the temperature gradient $\frac{dT}{dt}$ developed in the gage may be quite small mainly because of the large, thermal time constant of the gage. In other words, the pressure recording of the shock wave has taken place before the thermal effects modify the gage output. However, for pressure/time histories of 100 to 200 msec, the thermal effect may be evidenced by a slow increase, or decrease, in the true pressure-pulse level (where $T = \text{constant}$).

This thermal effect usually can be retarded by a thermal insulator such as a thin film of grease placed over the face of the gage. The thermal sensitivity is shown also to be a function of the gage construction. Nearly complete temperature isolation is possible by thermally insulating the gage.

Since many of the pressure pulses last a small interval (2 to 50 msec), the heat transfer to the sensor occurs after the information signal has been recorded. Figure 15 shows the variations in output for a lead metaniobate sensor (gage) for three different oven-controlled temperatures, 22° C., 47° C., and 63° C. Notice the linearity, Q/psi, has not been affected by operating at a different constant-temperature level.

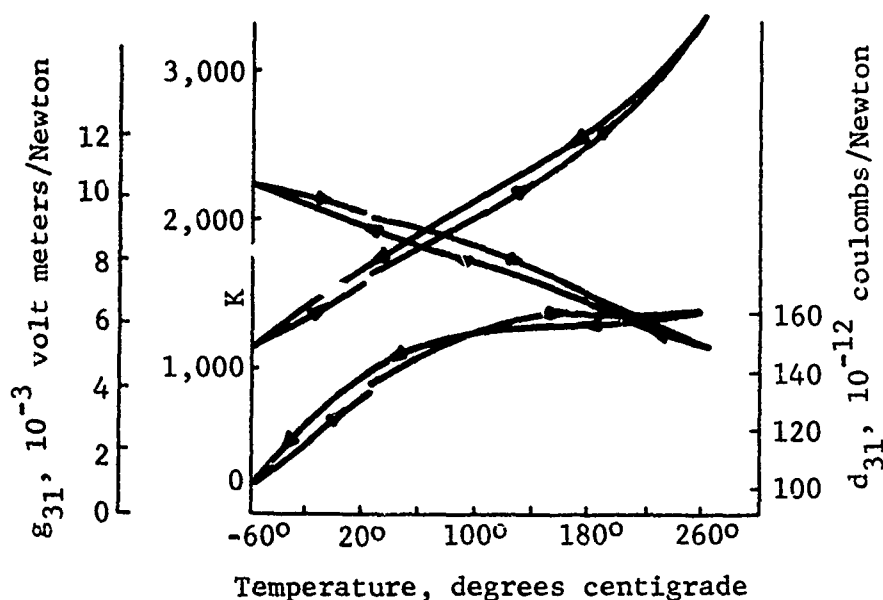


Figure 31. Temperature variation of the dielectric constant, K , and the piezoelectric strain constants, g_{31} and d_{31} , for PZT-5⁴

The change in output versus temperature is shown at a fixed pressure of 28.28 psi in figure 32. This shows the change $\Delta V/\Delta T$ to be approximately 0.77 mv per degree centigrade. In the area of the detonation chamber, the temperature gradients are very great and require gage shielding.

Temperature effects pose no serious problem provided the system is allowed to stabilize before testing takes place.

(h) Cabling.

Cable noise is readily apparent for low-level signals. With high-gain amplifier settings, it is only necessary to bend or strike the gage cable (connects gage to cathode follower) to observe a large spike in the output of the system. This effect is only important when the signal-to-noise ratio is low. Large

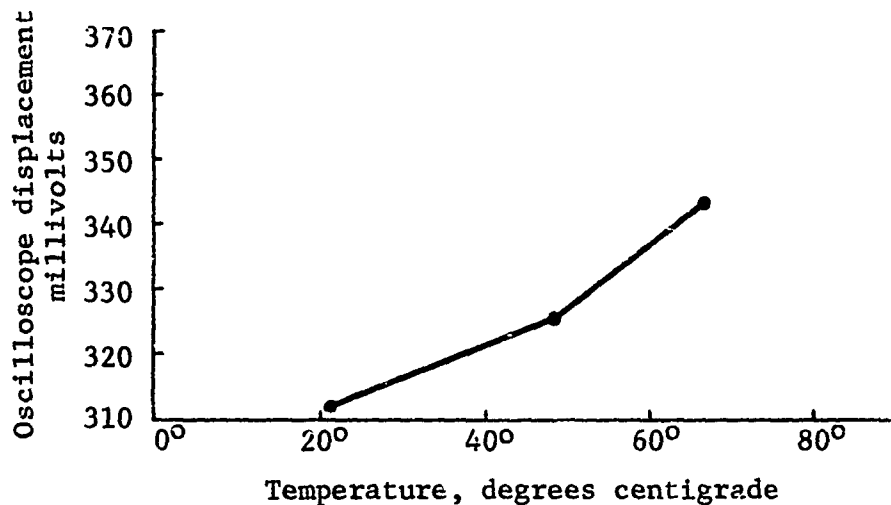


Figure 32. Oscilloscope displacement from pressure gage for constant pressure and different ambient temperatures

transducer outputs, pQ/psi, overshadow the noise so as to make these effects negligible. Such conditions are noted in figures 2, 3, 4, 11, 12, 22, and 23 where the signal-to-noise ratios S/N were much greater than unity.

For strain-gage measurements, the signal levels are usually in the range of 0 to 50 mv, and the cabling noise effects can be quite noticeable if the input leads, etc., are not properly shielded.

There are essentially three sources for noise generation by a cable, particularly when the cable is buried in soils and exposed to the shock wave. These sources are (1) the change in capacitance due to the cable being compressed by the shock wave; (2) the generation of static charge due to the rubbing of the cable insulation and shield; and (3) the presence of faulty connectors

on the cable (or faulty connections to the system).

For weak signals, the capacitance of the cable can be reduced by selecting low-capacitance cables or by using widely separated wires instead of a cable. Minimizing the amount of cable exposed to the shock wave reduces the capacitance effect. Placing the sensor into a saucer-type gage, where the signal is coupled directly to its preamplifier, eliminates the input cable entirely. Experimental packages have been fabricated which satisfy these requirements. See appendix B.

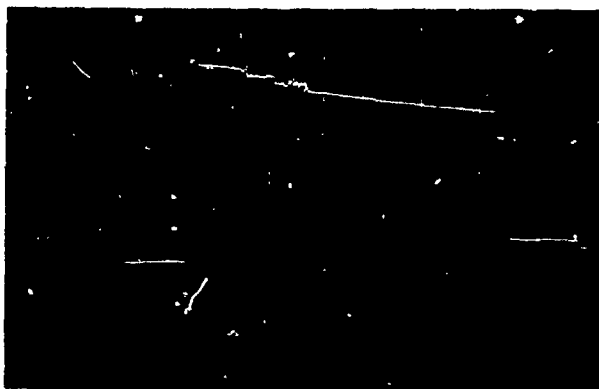
The use of special, processed cable* having graphite between the shield and the inside insulation provides a shorting path for accumulated static charge.

An example of the use of an intermittent cable connector is shown by the recorded pressure pulse from the tank calibrator in figure 33a. Compare this pulse with one of the proper pulses as shown in figures 13 and 14.

(i) Electrostatic effect.

An electrostatic effect that is associated primarily with the gage is the movement of electrostatic charge, or ionized particles, across the face of the gage. This effect can be demonstrated by mounting an open cable (gage removed) in a regular gage-mounting part in the shock tube. The cable end is made flush with the inside wall of the tube. The voltage induced in the cable due to the charge motion caused by the shock wave is shown in figure 33b. The test demonstrates that some of the noise is due to electrostatic effect. Even with the laboratory shock tube (used for calibrating gages) which has a smooth inside wall, there is an indication of some turbulence on all pressure-pulse recordings. This may not be turbulence but rather, in part, an electrostatic effect

* Microdot cable, manufactured by the Microdot Corporation.



Sweep: 50 msec/cm
Displacement: 0.2 v/cm

a. Pressure pulse from tank calibrator with faulty connector at gage



Sweep: 2 msec/cm
Displacement: 0.05 v/cm

b. Induced noise voltage from shock wave passing over open connector positioned in gaging station

Figure 33. Photographs showing (a) pressure pulse from tank calibrator with faulty connector at gage and (b) induced noise voltage from shock wave passing over open connector in gaging station

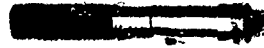
recorded by the piezoelectric sensor which modulates the true pressure pulse. Separation of these two effects is difficult and not conclusive.

To eliminate this condition, the gage can be encased in a complete metal housing; furthermore, where electrostatic conditions are suspected, it is only necessary to paint the gage with a conducting silver coating to provide a leakage path to ground.

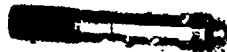
APPENDIX A PRESSURE GAGES



A POLYCRYSTALLINE MODIFIED
LEAD ZIRCONATE TITANATE, PZT-5



B EARLY TYPE BARIUM TITANATE



C POLYCRYSTALLINE MODIFIED
LEAD ZIRCONATE TITANATE, PZT-A



D BARIUM TITANATE



E PZT-5



F LEAD METANIIOBATE SENSOR



G LEAD METANIIOBATE SENSOR



H LEAD METANIIOBATE SENSOR



I TOURMALINE SENSOR



J QUARTZ SENSOR



K PIEZITE

APPENDIX B TRANSDUCERS

A POLYCRYSTALLINE WIRE IN
LEAD TEMPERATURE TRANSDUCER, RTT-1



B CANTY TYPING MACHINE TRANSDUCER



C POLYCRYSTALLINE WIRE IN
LEAD TEMPERATURE TRANSDUCER, RTT-1



D BATTERY TRANSDUCER



E RTT-1



F LEAD TEMPERATURE TRANSDUCER



G LEAD TEMPERATURE TRANSDUCER



H LEAD TEMPERATURE TRANSDUCER



I THERMAL TRANSDUCER



J GEMMA TRANSDUCER



K PISTON



PRESSURE GAGES

A WIRE TRANSDUCER



B WIRE TRANSDUCER



C CANTY TYPING MACHINE TRANSDUCER



D WIRE TRANSDUCER



DISPLACEMENT GAGES



WIRE TRANSDUCER

A WIRE TRANSDUCER

B WIRE TRANSDUCER

C WIRE TRANSDUCER

STRAIN GAGES

A PISTON



B PISTON



C PISTON



ACCELEROMETERS



A PISTON



SAUCER GAGES

SOIL PLACED
TRANSDUCERS

LOAD CELL

FORCE WASHER

TRANSDUCERS

REFERENCES

1. Modern Piezoelectric Components. Clevite Electronic Components, Div. of Clevite Corp., Cleveland, Ohio. Bull. No. 9244-1, Jan. 1962.
2. Jaffe, B. A Primer on Ferroelectricity and Piezoelectric Ceramics. Clevite Corp., Electronic Res. Div., Cleveland, Ohio, Eng. Memo No. 60-14, Dec. 1960.
3. IRE Standard on Piezoelectric Crystals: Measurements of Piezoelectric Ceramics. Proc. IRE, vol. 49, July 1961.
4. Berlincourt, D., Jaffe, B., Jaffe, H., and Krueger, H. A. Transducer Properties of Lead Titanate Zirconate Ceramics. Clevite Corp., Electronic Res. Div., Cleveland, Ohio. Reprint, IRE Natl. Conv. Rec., 1959.
5. American Standard Methods for the Calibration of Shock and Vibration Pickups. American Standards Assoc., Inc., Nov. 27, 1959.
6. Mason, W. P. Piezoelectric Crystals and Their Application to Ultrasonics. D. Van Nostrand Co., New York, N.Y., 1949.
7. Sanchez, J. C. Recent Developments in Flexible Silicon Strain Gages. ISA, Automation Conf., St. Louis, Mo., Jan. 17-19, 1961.
8. Crist, R. A., and Holt, R. E. Calibration of a Six-Foot- and a Two-Foot-Diameter Shock Tube. Kirtland Air Force Base, Albuquerque, N. Mex., AFSWC-TDR-63-5, 1963.
9. Sanchez, J. C., and Wright, W. V. Recent Developments in Flexible Silicon Strain Gages. ISA Paper 37-SL-61, St. Louis, Mo., Jan. 17-19, 1961.
10. Sanchez, J. C., and Wright, W. V. Recent Advances in Flexible Semi-conductor Strain Gages. ISA Paper 46-LA-61, Los Angeles, Calif., Sept. 11-15, 1961.
11. Frank, E. Strain Indicators for Semi-conductor Gages. ISA Paper 58-LA-61, Los Angeles, Calif., Sept. 11-15, 1961.
12. Valley, G. E., Jr., and Wallman, H. Vacuum Tube Amplifiers. MIT Rad. Lab. Series, vol. 18, McGraw-Hill Book Co., Inc., New York, N.Y., 1948.

REFERENCES (cont'd)

13. Wright, J. K. Shock Tubes (Ch. 1). Methuen and Co., Ltd., London; and John Wiley and Sons, Inc., New York, N.Y., 1961.
14. Durelli, A. J., and Riley, W. F. Initial Investigation of Wave Propagation in Large Soil Models. Armour Research Foundation, Chicago, Illinois (Kirtland Air Force Base, Albuquerque, N. Mex., AFSWC-TN-58-25, Dec. 1958).
15. Patterson, J. L. A Miniature Electrical Pressure Gage Utilizing a Stretched Flat Diaphragm. Natl. Advisory Committee for Aeronautics, Langley Aeronautical Lab., Langley Field, Va. Tech. Note 2659.
16. Bouche, R. R. High Frequency Response and Transient Motion Performance Characteristics of Piezoelectric Accelerometers. ISA Paper 50-LA-61, Los Angeles, Calif., Sept. 11-15, 1961.
17. Goldberg, H. Some Notes on Noise Figures. Proc. IRE vol. 36, Oct. 1948, pp. 1205-1214.

DISTRIBUTION

No. cys

HEADQUARTERS USAF

3 Hq USAF (AFOCE), Director of Civil Engineering, Wash, DC 20330
 1 Hq USAF (AFRNE-B), Wash, DC 20330
 1 USAF Dep, The Inspector General (AFIDI), Norton AFB, Calif
 1 USAF Directorate of Nuclear Safety (AFINS), Kirtland AFB, NM 87117
 1 AFCRL, Hanscom Field, Bedford, Mass 01731

MAJOR AIR COMMANDS

1 AFSC (SCT), Andrews AFB, Wash 25, DC
 1 AUL, Maxwell AFB, Ala 36112
 1 USAFIT (USAF Institute of Technology), Wright-Patterson AFB, Ohio 45443
 1 USAFA, United States Air Force Academy, Colo

AFSC ORGANIZATIONS

2 RTD (RTTR), Bolling AFB, Wash 25, DC
 1 BSD (BSR), Norton AFB, Calif 92409
 1 SSD, AF Unit Post Office, Los Angeles 45, Calif
 1 AF Msl Dev Cen (RRRT), Holloman AFB, NM 88330
 1 RADC (Document Library), Griffiss AFB, NY 13442

KIRTLAND AFB ORGANIZATIONS

1 AFSWC (SWEH), Kirtland AFB, NM 87117
 AFWL, Kirtland AFB, NM 87117
 50 WLL
 1 WLR
 35 WLRS
 1 WLX

ARMY ACTIVITIES

2 Director, Ballistic Research Laboratories (Library), Aberdeen Proving Ground, Md 21005
 2 Director, US Army Waterways Experiment Sta (WESRL), P. O. Box 631, Vicksburg, Miss

DISTRIBUTION (cont'd)

No. cys

NAVY ACTIVITIES

- 2 Commanding Officer and Director, Naval Civil Engineering Laboratory, Port Hueneme, Calif
- 1 Officer-in-Charge, Naval Civil Engineering Corps Officers School, US Naval Construction Battalion Center, Port Hueneme, Calif
- 1 Commanding Officer, US Naval Weapons Evaluation Facility (NWEF), Kirtland AFB, NM 87117

OTHER DOD ACTIVITIES

- Chief, Defense Atomic Support Agency, Wash 25, DC
- 1 Document Library, ATTN: Miss Gertrude Camp
- 1 DASABS, ATTN: Mr. J. Lewis
- 1 Commander, Field Command, Defense Atomic Support Agency (FCAG3, Special Weapons Publication Distribution), Sandia Base, NM 87115
- 20 Hq Defense Documentation Center for Scientific and Technical Information (DDC), Bldg 5, Cameron Sta, Alexandria, Va 22314

AEC ACTIVITIES

- 1 Sandia Corporation (Information Distribution Division), Box 5800, Sandia Base, NM 87115

OTHER

- 1 OTS, Department of Commerce, Wash 25, DC
- 1 MRD Division, General American Transportation Corp, 7501 North Natchez Ave, Niles 48, Ill
- 1 National Engineering Science Company, ATTN: Dr. Al Soldate, 711 South Fair Oaks Ave, Pasadena, Calif
- 1 Shannon & Wilson, Inc., Soil Mechanics & Foundation Engineers, ATTN: Mr. Stanley Wilson, 1105 North 38th St, Seattle 3, Wash
- 1 United Research Services, 1811 Trousdale Drive, Burlingame, Calif
- 2 University of Illinois, 111 Talbot Laboratory, Urbana, Ill
- 100 University of New Mexico, ATTN: Dr. Eugene Zwayer, Box 188, University Station, Albuquerque, NM
- 2 University of Notre Dame, Department of Civil Engineering, ATTN: Dr. Harry Saxe, Prof Leroy D. Graves, Notre Dame, Ind
- 1 Stanford Research Institute (Mr. F. Sauer), Menlo Park, Calif 94025

DISTRIBUTION (cont'd)

No cys

- 1 University of Washington, ATTN: Dr. I. M. Fyfe,
Seattle 5, Wash
- 1 Purdue University, Civil Engineering Dept, ATTN: Prof
G. A. Leonards, Lafayette, Ind
- 1 California Institute of Technology, ATTN: Dr. Paul J. Blatz,
1201 East California Blvd, Pasadena, Calif
- 1 Massachusetts Institute of Technology, Dept of Civil &
Sanitary Engineering, ATTN: Dr. Robert Whitman, 77
Massachusetts Ave, Cambridge 39, Mass
- 1 South Dakota School of Mines & Technology, ATTN: Dr.
Edwin H. Oshier, Rapid City, SD
- 1 Paul Weidlinger & Associates, ATTN: Dr. M. L. Baron,
770 Lexington Ave, New York 21, NY
- 2 Lovelace Foundation for Medical Education & Research, ATTN:
Dr. Clayton S. White, Director of Research, Dr. Donald R.
Richmond, 4800 Gibson Blvd, SE, Albuquerque, NM
- 1 The RAND Corporation, ATTN: Dr. Armas Laupa, 1700 Main St,
Santa Monica, Calif 90406
- 1 The MITRE Corporation, ATTN: Mr. Walter Gunter, P. O. Box
208, Bedford, Mass
- 4 The University of New Mexico, ATTN: Dean R. H. Clough,
Dr. Victor Skoglund, Prof Harold Walker, Dr. Thomas T.
Castonguay, Albuquerque, NM
- 1 Rice Institute of Technology, Dept of Civil Engineering, ATTN:
Dr. George Triandafilidis, Houston 1, Texas
- 1 Mr. Guy V. Martin, 110 Yale Blvd, SE, Albuquerque, NM
- 1 University of Michigan, Civil Engineering Dept, ATTN: Dr.
F. E. Richart, Jr., Ann Arbor, Mich
- 1 University of California, Civil Engineering Dept, ATTN:
Dr. H. Bolton Seed, Berkeley, Calif
- 1 University of Massachusetts, Civil Engineering Dept, ATTN:
Dr. Merit P. White, Amherst, Mass
- 1 Worcester Polytechnic Institute, Civil Engineering Dept,
Worcester, Mass
- 1 Kaman Nuclear Corp, ATTN: Dr. Burt Bittner, Colorado
Springs, Colo
- 1 Atlantic Research Corp, ATTN: Royal C. Bryant, Edsall Road
& Shirley Hwy, Alexandria, Va
- 6 Dr. Frank Janza, 1699 Silacci Drive, Campbell, Calif

DISTRIBUTION (cont'd)

No cys

- 6 University of New Mexico Library, Mr. Arthur L. DeVolder,
Technical Service Librarian, Serials Dept. Zimmerman Library,
University of New Mexico, Albuquerque, NM
- 1 Mr. Benjamin Granath, Susquehanna Instruments, Box 374,
R.D. 1, Bel Air, Md
- 1 Administrator, National Aeronautics and Space Administration,
1520 H Street, NW, Wash 25, DC
- 1 Space Technology Labs, Inc., ATTN: Technical Information
Center, Document Procurement, P. O. Box 95001, Los Angeles
45, Calif
- 1 IIT Research Institute, 3422 South Dearborn Street, Chicago 15.
Ill
- 5 University of New Mexico, ATTN: C. W. Hicks, Box 188,
University Station, Albuquerque, NM
- 1 University of Rhode Island, College of Engineering, ATTN:
Prof Vita A. Nacci, Kingston, RI
- 1 Howard Warshaw, Lockheed Missiles and Space Company,
Dept 58-11, Sunnyvale, Calif
- 1 Official Record Copy (Capt T. F. Dean, WLRS)